Relativistic models of magnetars: structure and deformations

A. Colaiuda,[1,2] V. Ferrari,[1]★ L. Gualtieri[1] and J. A. Pons[3]

[1]*Dipartimento di Fisica 'G. Marconi', Università di Roma 'La Sapienza' and Sezione INFN ROMA1, 00185 Roma, Italy*
[2]*Institut für Theoretische Physik, 72076 Tübingen, Germany*
[3]*Departament de Física Aplicada, Universitat d'Alacant, 03080 Alacant, Spain*

ABSTRACT

We find numerical solutions of the coupled system of Einstein–Maxwell equations with a linear approach, in which the magnetic field acts as a perturbation of a spherical neutron star. In our study, magnetic fields having both poloidal and toroidal components are considered, and higher order multipoles are also included. We evaluate the deformations induced by different field configurations, paying special attention to those for which the star has a prolate shape. We also explore the dependence of the stellar deformation on the particular choice of the equation of state and on the mass of the star. Our results show that, for neutron stars with mass $M = 1.4\,\mathrm{M}_\odot$ and surface magnetic fields of the order of 10^{15} G, a quadrupole ellipticity of the order of 10^{-6} to 10^{-5} should be expected. Low-mass neutron stars are in principle subject to larger deformations (quadrupole ellipticities up to 10^{-3} in the most extreme case). The effect of quadrupolar magnetic fields is comparable to that of dipolar components. A magnetic field permeating the whole star is normally needed to obtain negative quadrupole ellipticities, while fields confined to the crust typically produce positive quadrupole ellipticities.

Key words: gravitational waves – stars: magnetic fields – stars: neutron.

1 INTRODUCTION

The measured periods and spin down rates of soft-gamma repeaters (SGR) and of anomalous X-ray pulsars (AXP), and the observed X-ray luminosities of AXP, indicate that these neutron stars have extremely high magnetic fields, as large as 10^{14}–10^{15} G (Duncan & Thompson 1992; Thompson & Duncan 1993; Mereghetti & Stella 1995; Kouveliotou et al. 1999; Woods & Thompson 2006). Furthermore, if these sources are the central engine of gamma-ray bursts, as suggested in (Usov 1992; Kluzniak & Ruderman 1998; Wheeler et al. 2000), their magnetic field might even be larger. Up to now, about 10 highly magnetized neutron stars, the 'magnetars', have been identified in our Galaxy, but their actual number may be larger, and it has been suggested that a fraction of pulsars ($\gtrsim 10$ per cent, Kouveliotou et al. 1999) would possibly become magnetars at some stage of evolution. The discovery of magnetars has triggered a growing interest in the study of the structure, dynamics and evolution of neutron stars with large magnetic fields, and has raised a number of interesting issues. For example, quasiperiodic oscillations have been detected in the aftermath of the giant flares of SGR 1806−20 and SGR 1900+14, and it is not clear whether they are associated to crustal modes, or to modes of the magnetic field (or both); if the spacing between the observed frequencies would be explained, one may gain information on the internal structure of the star (Israel et al. 2005; Samuelsson & Andersson 2005; Strohmayer & Watts 2005; Sotani, Kokkotas & Stergioulas 2007).

In addition, magnetars may be interesting sources of gravitational waves, especially if they possess a toroidal magnetic field; indeed, as suggested by Jones and Cutler (Jones 1975; Cutler 2002), a large toroidal component tends to distort the star into a prolate shape, leading to a secularly unstable object: the wobble angle between the angular momentum and the star's magnetic axis would grow on a dissipation time-scale, until they become orthogonal. This may produce a copious flux of gravitational waves, potentially detectable by the advanced version of gravitational wave detectors LIGO and VIRGO (Cutler 2002).

In order to understand magnetars' structure and dynamics, it is necessary to model their equilibrium configuration in the framework of general relativity, including both poloidal and toroidal magnetic field components. Toroidal fields should form during the first seconds after core collapse, when the star is likely to be rapidly and differentially rotating: the fluid motion would drag the poloidal field lines creating large toroidal fields (Usov 1992; Kluzniak & Ruderman 1998; Wheeler et al. 2000); in addition, convective motions prevailing in the early life of a neutron star could also create toroidal fields by dynamo processes (Duncan & Thompson 1992; Thompson & Duncan 1993; Mereghetti & Stella 1995; Kouveliotou et al. 1999; Oron 2002; Bonanno & Rezzolla 2003). These toroidal components are expected to survive when the protoneutron star cools down and the crust forms. We also stress that large toroidal

★E-mail: valeria.ferrari@roma1.infn.it

components contribute to explain the giant flares in current models of SGRs (Duncan & Thompson 1992; Thompson & Duncan 1993; Mereghetti & Stella 1995; Kouveliotou et al. 1999). In Flowers & Ruderman (1977) it has been shown that a purely poloidal magnetic field is unstable, and decays on a time-scale much shorter than the star's life (see also Braithwaite & Spruit 2006 and references therein, and Pons & Geppert 2007); however, as discussed in (Braithwaite & Spruit 2006), a magnetic field configuration with prevailing toroidal component is also expected to be unstable on a short time-scale. Thus, both toroidal and poloidal magnetic fields have to be included to construct accurate, and stable, models of magnetars. Although these stability studies are Newtonian, we do not expect that General Relativistic analysis give different results.

In recent literature, magnetars equilibrium configurations have been studied by solving Einstein–Maxwell equations, coupled with the hydrodynamics equations, in full general relativity (Boquet et al. 1995; Bonazzola & Gourgoulhon 1996; Cardall et al. 2001). However, the numerical schemes used in most cases require circularity of the space–time, i.e. the existence of two hypersurface-orthogonal Killing vectors, and this assumption automatically excludes fields with both poloidal and toroidal components, since they break circularity. Therefore, in (Boquet et al. 1995; Bonazzola & Gourgoulhon 1996; Cardall et al. 2001) only poloidal magnetic fields have been considered.

A different approach has been used in Ioka & Sasaki (2004) and Konno, Obata & Kojima (1999); Konno et al. (2000), where equilibrium configurations have been studied using a perturbative techniques, i.e. solving Einstein–Maxwell hydrodynamics equations, linearized about a spherically symmetric background, and expanding the perturbed equations in tensor harmonics. Toroidal fields have been included in the analysis only in Ioka & Sasaki (2004), but this work is based on very restrictive assumptions: the magnetic field is assumed to vanish outside the star. Poloidal and toroidal fields have also been considered in the framework of Newtonian gravity in a recent work (Yoshida & Eriguch 2006; Yoshida et al. 2006; Haskell et al. 2007).

In this paper we construct equilibrium configurations of neutron stars with strong magnetic fields in general relativity. Since magnetars rotate very slowly, we restrict to non-rotating stars. However, rotation can play an important role in the early phases of the stellar evolution; therefore, it will be included in future developments of this work. We follow a perturbative approach, generalizing the work of Konno et al. (1999) to include toroidal magnetic fields, with a magnitude comparable with that of the poloidal fields. We start solving the relativistic Grad–Shafranov equation, to which Maxwell equations can be reduced, in the background of a non-rotating star; we impose a set of boundary conditions which correspond to different magnetic field configurations, and construct the corresponding stress–energy tensor. The magnetic field perturbs the star, which is consequently deformed; to compute the stellar structure and its deformation, we then solve the Einstein–Maxwell hydrodynamics equations linearized about the spherically symmetric background of the non-rotating star, having the electromagnetic and the fluid stress–energy tensors as a source. We compare the deformation induced by a magnetic field with that which would be produced by rotation, and find that effect of magnetic fields is dominant for magnetars as SGR and AXP. We discuss how the magnetic field profile and the corresponding stellar deformation depend on the stellar mass and on the equation of state (EOS) of the fluid composing the star, comparing different stellar models. In current literature, only the $l = 1$ multipole of the electromagnetic potential is usually considered. In this paper we also solve the relevant equations for the $l = 2$ multipole.

The main features of the perturbative approach are described in Section 2. The results of the numerical integrations of the relativistic Grad–Shafranov equation, and of the equations of stellar perturbations, are reported and commented in Section 3 for different field configurations and different stellar models. In Section 3 we also discuss the effects of the $l = 2$ multipole. Conclusions are drawn in Section 4.

2 STRUCTURE OF A STATIONARY, AXISYMMETRIC NEUTRON STAR WITH POLOIDAL AND TOROIDAL MAGNETIC FIELDS

In what follows we shall assume that the magnetized fluid composing the non-rotating neutron star can be described within the framework of ideal magnetohydrodynamics (MHD), i.e. that there is no separation of charge currents flowing through the star. It should be mentioned that, although this assumption is appropriate inside the fluid core, it may not apply to the stellar solid crust. The magnetic field and the deformation it induces on the star are treated as stationary and axisymmetric perturbations of a spherically symmetric background. We consider perturbations up to order $O(B^2)$. We shall follow the notation and the formalism introduced in Konno et al. (1999), generalized to include toroidal magnetic fields.

Before proceeding with the perturbative approach, in the next subsection we shall summarize some general properties of stationary, axisymmetric magnetized stars, which will be useful in subsequent sections. These properties and their proofs can be found in the literature, but are scattered in different papers (Carter 1973; Bekenstein & Oron 1978; Bekenstein & Oron 1979; Ioka & Sasaki 2003); here we report them in a unified and consistent way.

2.1 Some properties of stationary, axially symmetric magnetized stars

We consider a stationary, axisymmetric space–time describing a magnetized star, with coordinates

$$x^\mu = (t, x^a, \phi) \quad (a = 1, 2), \tag{1}$$

where $\eta = \partial/\partial t$ and $\xi = \partial/\partial \phi$ are Killing vectors. The coordinates x^a can be, for instance, spherical coordinates (r, θ), or cylindrical coordinates (r, z). Any stationary, axisymmetric quantity, such as the vector potential or the fluid 4-velocity, are independent of t and ϕ, i.e. $A_\mu = A_\mu(x^a), u^\mu = u^\mu(x^a)$.

The electric and magnetic field are defined as

$$E_\mu \equiv F_{\mu\nu} u^\nu, \quad B_\mu \equiv -\frac{1}{2} \epsilon_{\alpha\beta\gamma\delta} u^\beta F^{\gamma\delta}, \tag{2}$$

where $F_{\mu\nu} \equiv \partial_\mu A_\nu - \partial_\nu A_\mu$. It may be noted that since $\partial_t A_\mu = \partial_\phi A_\mu = 0$, $F_{t\phi} = 0$. We define the local angular velocity of the fluid as

$$\Omega(x^a) \equiv \frac{\mathrm{d}\phi}{\mathrm{d}t} = \frac{u^\phi}{u^t}. \tag{3}$$

The components u^a of the fluid velocity are called *meridional currents*. Furthermore, we define the quantities

$$\Phi(x^a) \equiv \eta^\mu A_\mu = A_t, \quad \Psi(x^a) \equiv \xi^\mu A_\mu = A_\phi. \tag{4}$$

The ideal MHD hypothesis implies that the electric field, measured by a comoving observer, vanishes:

$$E_\mu = F_{\mu\nu} u^\nu = 0. \tag{5}$$

An axially symmetric magnetic field is *poloidal* if its non-vanishing space components are

$$(B^a, 0) \, ; \tag{6}$$

it is *toroidal* if

$$\left(0, 0, B^\phi\right) . \tag{7}$$

2.1.1 Vanishing meridional currents

If meridional currents vanish $u^a = 0$, and equation (5) gives

$$E_a = F_{at}u^t + F_{a\phi}u^\phi = (F_{at} + \Omega F_{a\phi})u^t = 0$$
$$\Rightarrow \frac{F_{1t}}{F_{2t}} = \frac{F_{1\phi}}{F_{2\phi}} = -\Omega . \tag{8}$$

As $F_{at} = \partial_a \Phi$ and $F_{a\phi} = \partial_a \Psi$, equation (8) becomes

$$\partial_a \Phi = -\Omega \partial_a \Psi . \tag{9}$$

Furthermore, from (8) we have

$$\partial_1 \Phi \partial_2 \Psi - \partial_2 \Phi \partial_1 \Psi = 0, \tag{10}$$

which implies (assuming the domain where Φ and Ψ are defined is simply connected) that $\Phi = \Phi(\Psi)$. From equation (9) then it follows that

$$\frac{d\Phi}{d\Psi} = -\Omega . \tag{11}$$

As shown by Carter (see theorem 7 of Carter 1973, and its corollary; see also Bonazzola et al. 1993), if the space–time is stationary and axisymmetric, and if meridional currents are zero, then $A_a = 0$. Therefore, the vector potential is

$$A_\mu = (\Phi, 0, 0, \Psi), \tag{12}$$

the electromagnetic tensor becomes

$$F_{\mu\nu} = \begin{pmatrix} 0 & \Omega\Psi_{,a} & 0 \\ -\Omega\Psi_{,a} & 0 & \Psi_{,a} \\ 0 & -\Psi_{,a} & 0 \end{pmatrix}, \tag{13}$$

and the magnetic field is

$$B^\alpha = \epsilon^{\alpha\beta\mu\nu} u_\beta F_{\mu\nu} = (0, B^a, 0) , \tag{14}$$

since $g^{at} = g^{a\phi} = 0$ when $u^a = 0$ (Carter 1973). Thus, if meridional currents vanish the magnetic field is poloidal.

2.1.2 Non-vanishing meridional currents

Let us now consider the general case $u^a \neq 0$. Equation (5) gives

$$E_t = F_{ta}u^a = -u^a\partial_a\Phi = -u^\mu\partial_\mu\Phi = -\frac{d\Phi}{d\tau} = 0$$
$$E_\phi = F_{\phi a}u^a = -u^a\partial_a\Psi = -u^\mu\partial_\mu\Psi = -\frac{d\Psi}{d\tau} = 0, \tag{15}$$

i.e. Φ, Ψ are constant along the fluid flow. Then

$$\begin{aligned} u^1\Phi_{,1} + u^2\Phi_{,2} &= 0 \\ u^1\Psi_{,1} + u^2\Psi_{,2} &= 0, \end{aligned} \tag{16}$$

which implies $\Phi = \Phi(\Psi)$. We introduce the quantity

$$\bar{\Omega}(\Psi) \equiv -\frac{d\Phi}{d\Psi}, \tag{17}$$

so that

$$\partial_a \Phi = -\bar{\Omega}\partial_a \Psi . \tag{18}$$

Note that in general $\bar{\Omega} \neq \Omega$. Indeed

$$\begin{aligned} E_a &= -(\partial_a\Phi + \Omega\partial_a\Psi)u^t + F_{ab}u^b \\ &= (\bar{\Omega} - \Omega)\partial_a\Psi u^t + F_{ab}u^b = 0 \qquad a, b = 1, 2; \end{aligned} \tag{19}$$

thus, if $F_{ab} \neq 0$, then $\bar{\Omega} \neq \Omega$.

From equation (16) it also follows that

$$\Psi_{,2} = -\frac{u^1}{u^2}\Psi_{,1}, \tag{20}$$

which, differentiated with respect to x^1, gives

$$-\left(\frac{u^1}{u^2}\right)_{,1} \Psi_{,1} = \frac{u^a}{u^2}\partial_a\Psi_{,1}. \tag{21}$$

Using the *continuity equation*

$$u^\alpha_\alpha = -\frac{d}{d\tau}\ln(\sqrt{-g}n), \tag{22}$$

where n is the baryon number density, equation (21) can be transformed as follows:

$$\begin{aligned} \frac{d}{d\tau}\ln(\Psi_{,1}) &= u^a\partial_a\ln(\Psi_{,1}) = -u^2\left(\frac{u^1}{u^2}\right)_{,1} \\ &= -u^\alpha_\alpha + \frac{u^\alpha u^2_{,\alpha}}{u^2} = \frac{d}{d\tau}\ln(nu^2\sqrt{-g}). \end{aligned} \tag{23}$$

If we now define

$$C \equiv \frac{\Psi_{,1}}{nu^2\sqrt{-g}}, \tag{24}$$

we find

$$\frac{d}{d\tau}C = u^a C_{,a} = 0 \quad \Rightarrow \quad u^1 C_{,1} + u^2 C_{,2} = 0, \tag{25}$$

which, together with equation (20) implies that C is a function of Ψ only, i.e. $C = C(\Psi)$.

By replacing $\Psi_{,1} = C(\Psi)nu^2\sqrt{-g}$ in equation (19) we find

$$F_{12} = -(\bar{\Omega} - \Omega)Cnu^t\sqrt{-g}. \tag{26}$$

Then, if Ω and $\bar{\Omega}$ do not coincide, $F_{12} \neq 0$; consequently, the magnetic field has both poloidal and toroidal components.

A possible interpretation of $\bar{\Omega}$ is the following (see e.g. Ioka & Sasaki 2004). From equation (26) we find

$$\Omega = \bar{\Omega} + \frac{F_{12}}{Cnu^t\sqrt{-g}},$$

from which we see that the fluid angular velocity Ω has two contributions: the first, $\bar{\Omega}$, can interpreted as due to the stellar rotation, the second is clearly due to the electromagnetic field. Although this interpretation is purely conventional, since we are considering a non-rotating star, we shall assume $\bar{\Omega} = 0$, and consequently $A_0 = \Phi = 0$. Thus the form of the vector potential is

$$A_\mu(r, \theta) = (0, A_r, A_\theta, \Psi) . \tag{27}$$

2.1.3 Electromagnetic current and Lorentz force

The Lorentz force is defined as

$$f_\mu \equiv F_{\mu\nu}J^\nu, \tag{28}$$

where the electromagnetic current J^μ is given by

$$J^\mu = \frac{1}{4\pi\sqrt{-g}}(\sqrt{-g}\,F^{\mu\nu})_{,\nu}. \tag{29}$$

The stress–energy tensor of a perfect fluid with an electromagnetic field is

$$T^{\mu\nu} = T^{\mu\nu}_{\text{fluid}} + T^{\mu\nu}_{\text{em}}, \tag{30}$$

where

$$T^{\mu\nu}_{\text{fluid}} = (\rho + p)u^\mu u^\nu + pg^{\mu\nu},$$

$$T^{\mu\nu}_{\text{em}} = \frac{1}{4\pi}\left(F^{\mu\alpha}F^\nu_{\ \alpha} - \frac{1}{4}g^{\mu\nu}F^{\rho\sigma}F_{\rho\sigma}\right). \tag{31}$$

By projecting the equation $T^{\mu\nu}_{\ ;\nu} = 0$ orthogonally to u^μ, we find the relativistic Euler equation in presence of a magnetic field:

$$(\rho + p)a_\mu + p_{,\mu} + u_\mu u^\nu p_{,\nu} - f_\mu = 0, \tag{32}$$

where $a_\mu = u^\nu u_{\mu;\nu}$. Let us now consider the ϕ component of this equation. Under the stationarity and axisymmetry assumption it becomes

$$(\rho + p)a_\phi + u_\phi u^a p_{,a} - f_\phi = 0; \tag{33}$$

being

$$a_\phi = u^\mu u_{\phi;\mu} = u^a u_{\phi,a} - u^\mu u^\nu \Gamma_{\phi\mu\nu}$$

$$= u^a u_{\phi,a} + \frac{1}{2}u^\mu u^\nu g_{\mu\nu,\phi} = u^a u_{\phi,a}, \tag{34}$$

using the first law of thermodynamics, $u^a p_{,a} = \frac{\rho+p}{n}u^a n_{,a}$, equation (33) gives

$$f_\phi = \frac{\rho + p}{n}u^a(nu_\phi)_{,a}. \tag{35}$$

If meridional currents are zero, $f_\phi = 0$.

2.2 The equations for the vector potential A^μ

The background geometry of the star in coordinates (t, r, θ, ϕ) is

$$ds^2 = -e^{\nu(r)}dt^2 + e^{\lambda(r)}dr^2 + r^2(d\theta^2 + \sin^2\theta\,d\phi^2)$$

$$= g^{(0)}_{\mu\nu}dx^\mu dx^\nu, \tag{36}$$

$$u^{(0)\mu} = (e^{-\nu/2}, 0, 0, 0), \tag{37}$$

where $\nu(r), \lambda(r)$ are the solution of Einstein equations for an assigned EOS. If a magnetic field is present, from the expression of $F_{\mu\nu}$ in terms of the electric and magnetic field $F_{\mu\nu} = u_\mu E_\nu - u_\nu E_\mu + \epsilon_{\mu\nu\alpha\beta}u^\alpha B^\beta$ we see that, if $E_\mu = 0$, then $F_{\mu\nu} = O(B)$; consequently, also the vector potential A_μ is of order $O(B)$. By using a function $\Lambda(r, \theta)$ such that $\Lambda_{,\theta} = A_\theta$, we can gauge away the θ component of the vector potential (27). By introducing the function $\Sigma(r, \theta) \equiv e^{(\nu-\lambda)/2}(A_r - \Lambda_{,r})$, it then becomes

$$A_\mu = (0, e^{(\lambda-\nu)/2}\Sigma, 0, \Psi), \tag{38}$$

with Σ and Ψ of order $O(B)$.

The magnetic field induces motion in the fluid, and consequently induces a perturbation on the components of the 4-velocity δu^α, on the pressure and energy density (δp and $\delta\rho$, respectively), and on the metric $\delta g_{\mu\nu}$. Since $T^{\mu\nu}_{\text{em}} = O(B^2)$, linearizing the equation $T^{\mu\nu}_{\ \nu} = 0$ (and using the vanishing of the space components of u^α when the magnetic field is absent), it is easy to see that $\delta u^\alpha = \delta p = \delta\rho = O(B^2)$. In a similar way, from the linearized Einstein equations it can be shown that $\delta g_{\mu\nu} = O(B^2)$. Thus, from equation (35) we see

that, since $\delta u^a = O(B^2)$, the ϕ-component of the Lorentz force is $f_\phi = O(B^4)$ and for this reason hereafter we shall set it equal to zero. This condition will be used to further simplify the expression of the vector potential. We stress that the condition $f_\phi = 0$ comes from the fact that $f_\phi = O(B^4)$, but we do not assume that meridional currents are zero. If we compute f_ϕ from Maxwell equations and impose $f_\phi = 0$ we find

$$f_\phi = (\Sigma_{,\theta\theta} + \cot\theta\,\Sigma_{,\theta})\Psi_{,r} - \Sigma_{,\theta r}\Psi_{,\theta} = 0, \tag{39}$$

therefore, if we define

$$\bar{\Psi} \equiv \sin\theta\,\Sigma_{,\theta}, \tag{40}$$

we have $\bar{\Psi}_{,\theta}\Psi_{,r} - \bar{\Psi}_{,r}\Psi_{,\theta} = 0$; this equation implies $\bar{\Psi} = \bar{\Psi}(\Psi)$, and consequently, since $\bar{\Psi} = O(B)$ and $\Psi = O(B)$, we can write $\bar{\Psi} = \zeta\Psi$, where ζ is a constant of order $O(1)$. The equation

$$\zeta\Psi = \sin\theta\,\Sigma_{,\theta} \tag{41}$$

is satisfied by

$$\Sigma = \zeta a$$
$$\Psi = \sin\theta\,a_{,\theta}, \tag{42}$$

with $a = a(r, \theta)$. Thus, the vector potential can be written as

$$A_\mu = \left(0, \zeta e^{(\lambda-\nu)/2}a, 0, \sin\theta\,a_{,\theta}\right). \tag{43}$$

As a consequence, the magnetic field takes the following form:

$$B_\mu = \frac{e^{-\lambda/2}}{\sin\theta}\left(0, \frac{e^\lambda}{r^2}(\sin\theta\,a_{,\theta})_{,\theta}, -(\sin\theta\,a_{,\theta})_r, \right.$$
$$\left. -\zeta\sin^2\theta e^{(\lambda-\nu)/2}a_{,\theta}\right). \tag{44}$$

From this expression we see that the coefficient ζ (or the dimensionless quantity ζR, where R is the radius of the star) represents the ratio between the toroidal and the poloidal components of the magnetic field. Since, as discussed in Section 1, a magnetic field configuration with prevailing toroidal component is expected to be unstable, we will not consider configurations with $\zeta R \gg 1$.

Assuming the form (43) of the vector potential, we find (neglecting the metric perturbations, which contribute to higher orders of B)

$$f_a = (\sin\theta\,a_{,\theta})_{,a}\frac{\tilde{J}_\phi}{r^2\sin^2\theta}, \tag{45}$$

where

$$\tilde{J}_\phi \equiv J_\phi - \zeta^2\frac{e^{-\nu}}{4\pi}\sin\theta\,a_{,\theta}. \tag{46}$$

We shall now show that f_a can be written as $(\rho + p)$ times the gradient of a function of (r, θ). Let us consider the a-components of Euler equation:

$$(\rho + p)a_a + p_{,a} + u_a u^b p_{,b} - f_a = 0. \tag{47}$$

We remind that

$$u^i \equiv \delta u^i = O(B^2), \quad g^{0i} \equiv \delta g^{0i} = O(B^2),$$
$$f_a = F_{a\mu}J^\mu = O(B^2).$$

Consequently, the term $u_a u^b p_{,b}$ is $O(B^4)$. We shall now compute a_a and $p_{,a}$ up to terms of order $O(B^2)$.

The acceleration is

$$a_a = u^\mu u_{a;\mu} = u^b u_{a,b} - u^\mu u^\nu \Gamma_{a\mu\nu} \simeq \frac{1}{2}u^\mu u^\nu g_{\mu\nu,a}$$

$$= \frac{1}{2}\left[(u^0)^2 g_{00,a} + 2u^0 u^i g_{0i,a} + u^i u^j g_{ij,a}\right]$$

$$\simeq \frac{1}{2}(u^0)^2 g_{00,a}. \tag{48}$$

We also find

$$g_{\mu\nu}u^\mu u^\nu = -1$$
$$= (u^0)^2 g_{00} + 2u^0 u^i g_{0i} + u^i u^j g_{ij} \simeq (u^0)^2 g_{00}, \tag{49}$$

then

$$a_a = \frac{1}{2}\left(\ln(-g_{00})\right)_{,a}. \tag{50}$$

From the first principle of thermodynamics, written for a barotropic EOS $p = p(\rho)$, we find

$$p_{,a} = (\rho + p)\left(\ln\frac{\rho + p}{n}\right)_{,a}. \tag{51}$$

If we introduce the function

$$\chi = \ln\left(\sqrt{-g_{00}}\frac{\rho + p}{n}\right), \tag{52}$$

using equations (45), (50) and (51), equation (47) becomes

$$(\rho + p)\chi_{,a} = (\sin\theta a_{,\theta})_{,a}\frac{\tilde{J}_\phi}{r^2\sin^2\theta}. \tag{53}$$

This equation is equivalent to equation (12) of Boquet et al. (1995). From (53) we find

$$\chi_{,12} - \chi_{,21} = (\sin\theta a_{,\theta})_{,1}\left(\frac{\tilde{J}_\phi}{r^2\sin^2\theta(\rho + p)}\right)_{,2}$$
$$- (\sin\theta a_{,\theta})_{,2}\left(\frac{\tilde{J}_\phi}{r^2\sin^2\theta(\rho + p)}\right)_{,1} = 0, \tag{54}$$

hence

$$\frac{\tilde{J}_\phi}{r^2\sin^2\theta(\rho + p)} = F(\sin\theta a_{,\theta}). \tag{55}$$

By expanding in powers of B we find

$$\frac{\tilde{J}_\phi}{r^2\sin^2\theta\left(\rho^{(0)} + p^{(0)}\right)} = c_0 + c_1\sin\theta a_{,\theta} + O(B^2), \tag{56}$$

thus, the ϕ component of the electromagnetic current can be written as follows:

$$J_\phi = \zeta^2\frac{e^{-\nu}}{4\pi}\sin\theta a_{,\theta}$$
$$+ [c_0 + c_1\sin\theta a_{,\theta}]\left(\rho^{(0)} + p^{(0)}\right)r^2\sin^2\theta + O(B^2). \tag{57}$$

In the next section we will expand $a(r, \theta)$ in Legendre polynomials; if we assume $c_1 \neq 0$, different harmonic components of the field couple. Following Ioka & Sasaki (2004), Konno et al. (1999), Konno et al. (2000), Haskell et al. (2007), hereafter we shall assume $c_1 = 0$. With this simplification,

$$J_\phi = \zeta^2\frac{e^{-\nu}}{4\pi}\sin\theta a_{,\theta} + c_0\left(\rho^{(0)} + p^{(0)}\right)r^2\sin^2\theta, \tag{58}$$

where c_0 is a constant of order $O(B)$. The r, θ components of the current are simply

$$J_a = \frac{\zeta e^{-(\lambda+\nu)/2}}{4\pi\sin\theta}\left(-\frac{e^\lambda}{r^2}(\sin\theta a_{,\theta})_{,\theta}, (\sin\theta a_{,\theta})_{,r}\right). \tag{59}$$

The electromagnetic current is the sum of two parts:

$$J_\mu = J_\mu^p + J_\mu^t \tag{60}$$

with

$$J_\mu^p = \left(0, 0, 0, c_0 r^2\sin^2\theta\left(\rho^{(0)} + p^{(0)}\right)\right)$$
$$J_\mu^t = -\frac{\zeta e^{-\nu/2}}{4\pi}B_\mu. \tag{61}$$

J_μ^p is the source of the poloidal field (which does not depend on ζ); J_μ^t is the source of the toroidal field (proportional to ζ) and it is parallel to the magnetic field. Note that

(i) since $J_\mu^t \propto B^\mu$, it follows that $F_{\mu\nu}J^{t\nu} = 0$;

(ii) when $J_\mu^p = 0$ (i.e. when $c_0 = 0$), then $f_\mu = F_{\mu\nu}J^\nu = 0$; therefore in this case the magnetic field is *force-free*.

If outside the star we assume there is vacuum, currents must vanish. As the poloidal current is proportional to $\rho^{(0)} + p^{(0)}$, it automatically vanishes; conversely, the toroidal current vanishes only if $\zeta = 0$, i.e. if the toroidal field vanishes. Therefore, in vacuum only poloidal fields (with no current) are allowed.

If outside the star there is a magnetosphere, the situation is different because currents can be present, and consequently toroidal fields can exist, and also because the ideal MHD assumption breaks down. In any event, since the matter density in the magnetosphere is very low, any significant Lorentz force would result in a large acceleration acting on the particles and disrupting the configuration, unless the magnetic field is very close to a force-free solution.

2.3 The relativistic Grad–Shafranov equation

If we expand the function $a(r, \theta)$ in Legendre polynomials,

$$a(r, \theta) = \sum_{l=1}^\infty a_l(r)P_l(\theta), \tag{62}$$

the vector potential (43) and the magnetic field (44) become

$$A_\mu = \left(0, \zeta e^{(\lambda-\nu)/2}\sum_l a_l P_l, 0, \sum_l a_l\sin\theta P_{l,\theta}\right)$$

$$B_\mu = \sum_l\left(0, -\frac{e^{\lambda/2}}{r^2}l(l+1)a_l P_l, -e^{-\lambda/2}a_{l,r}P_{l,\theta},\right. \tag{63}$$

$$\left.-\zeta e^{-\nu/2}a_l\sin\theta P_{l,\theta}\right). \tag{64}$$

From Maxwell equations we find $J_\phi = \frac{1}{4\pi}F_{\phi\ ;\mu}^{\ \mu}$, which gives

$$J_\phi = -\frac{1}{4\pi}\sin\theta\sum_l P_{l,\theta}\left(e^{-\lambda}a_{l,rr} + \frac{\nu_{,r} - \lambda_{,r}}{2}e^{-\lambda}a_{l,r}\right.$$
$$\left.-\frac{l(l+1)}{r^2}a_l\right). \tag{65}$$

Using the expansion (62), equation (58) gives

$$J_\phi = \zeta^2\frac{e^{-\nu}}{4\pi}\sum_l a_l\sin\theta P_{l,\theta} + c_0(\rho + p)r^2\sin^2\theta$$

$$= \zeta^2\frac{e^{-\nu}}{4\pi}\sum_l\sin\theta a P_{l,\theta} - c_0(\rho + p)r^2\sin\theta P_{1,\theta}. \tag{66}$$

Note that the poloidal current (i.e. the term in c_0) introduces an $l = 1$ dipole component. The linearized relativistic Grad–Shafranov equation (Ioka & Sasaki 2004) is found by equating equations (65) and (66) (see also Konno et al. 1999):

$$e^{-\lambda}a_1'' + \frac{\nu' - \lambda'}{2}e^{-\lambda}a_1' + \left(\zeta^2 e^{-\nu} - \frac{2}{r^2}\right)a_1$$
$$= 4\pi(\rho + p)r^2 c_0, \tag{67}$$

$$e^{-\lambda}a_l'' + \frac{\nu' - \lambda'}{2}e^{-\lambda}a_l' + \left(\zeta^2 e^{-\nu} - \frac{l(l+1)}{r^2}\right)a_l$$
$$= 0 \quad (l > 1). \tag{68}$$

Hereafter we will consider only the solution of equation (67) corresponding to $l = 1$, in which case the vector potential (64) and the magnetic field (64) become

$$
A_\mu = \left(0, \zeta e^{(\lambda - \nu)/2} a_1 \cos\theta, 0, -a_1 \sin^2\theta \right)
$$

$$
B_\mu = \left(0, -2\frac{e^{\lambda/2}}{r^2} a_1 \cos\theta, e^{-\lambda/2} a_1' \sin\theta, \right. \tag{69}
$$

$$
\left. \zeta e^{-\nu/2} a_1 \sin^2\theta \right). \tag{70}
$$

It is convenient to express the magnetic field in terms of the orthonormal tetrad components (i.e. those measured in a locally inertial frame) in the background metric (36), i.e.

$$
B_{(r)} = -\frac{2a_1}{r^2} \cos\theta, \tag{71}
$$

$$
B_{(\theta)} = \frac{e^{-\lambda/2} a_1'}{r} \sin\theta, \tag{72}
$$

$$
B_{(\phi)} = \zeta \frac{e^{-\nu/2} a_1}{r} \sin\theta. \tag{73}
$$

2.4 Boundary conditions and matching with the exterior

Different choices of the boundary conditions and of the matching conditions of the interior and exterior solutions of the Grad–Shafranov equation, correspond to different physical configurations. We shall consider the following cases.

(i) Magnetic field extending throughout the star. This configuration has been studied in the literature in several papers (e.g. in Konno et al. 1999; Ioka & Sasaki 2004); however, it conflicts with the common belief that the neutron star core is superconductor. Actually, if the superconductor is of type II, the magnetic field extends throughout the star, but it has a very complicated structure (it is 'quantized' in flux tubes). In type II superconductors the Lorentz force vanishes and is replaced by the flux-tube tension. A correct formalism describing the superfluid MHD equations is still under debate. Thus, the smooth magnetic field we consider in this paper is a rough representation of such configuration.

If we impose a regular behaviour at the origin [which implies $a_1(r \simeq 0) = \alpha_0 r^2 + O(r^4)$], for each pair of assigned constants α_0, c_0 the solution $a_1(r)$ is unique.

(ii) Crustal fields. If matter in the core is a type I superconductor, the magnetic field will be arranged in macroscopic (non-quantized) flux tubes and gradually expelled from the core depending on which is the configuration that minimizes the system energy. In this case, it may happen that the magnetic field is eventually entirely confined in the crust, i.e. within

$$
r_c \leqslant r \leqslant R, \tag{74}
$$

where r_c is the inner boundary of the crust and R is the stellar radius. We choose $r_c = 0.9R$. By imposing a regular behaviour near r_c, i.e. $a_1(r \gtrsim r_c) = \alpha_0(r - r_c) + O((r - r_c)^2)$, for each pair of assigned constants α_0, c_0 the solution $a_1(r)$ is unique.

We shall assume that outside the star there is vacuum, currents vanish and $\zeta = 0$ (see equation 58). Equation (67) then reduces to

$$
\left(1 - \frac{2M}{r} \right) a_1'' + \frac{2M}{r^2} a_1' - \frac{2}{r^2} a_1 = 0; \tag{75}
$$

its general solution (decaying at infinity) is a pure dipole:

$$
a_1(r) = -\frac{3\mu}{8M^3} r^2 \left[\ln\left(1 - \frac{2M}{r} \right) + \frac{2M}{r} + \frac{2M^2}{r^2} \right], \tag{76}
$$

where the constant μ is the magnetic dipole moment in geometrical units. The corresponding magnetic field has the form

$$
B_\mu = \left(0, -2\frac{e^{\lambda/2}}{r^2} a_1 \cos\theta, e^{-\lambda/2} a_1' \sin\theta, 0 \right). \tag{77}
$$

On the surface of the star, the function $a_1(r)$ solution of equation (67) has to be matched with the exterior solution (76), imposing the continuity of a_1 and a_1'. The ratio α_0/c_0 is fixed by matching the quantity a_1'/a_1 (which does not depend on μ). Once this ratio has been determined, the constants α_0, c_0 are rescaled by a common factor, which changes the constant μ (and then the global normalization of the field) by the same amount. We fix this constant by assuming that the magnetic field at the pole is $B_{\text{pole}} = 10^{15}$ G. In this way, for each assigned value of ζ we determine α_0 and c_0.

In previous papers on magnetized stars (Ioka & Sasaki 2004; Haskell et al. 2007), boundary conditions have been imposed in such a way that not only the toroidal, but also the poloidal component of the magnetic field vanishes outside the star; as a consequence, the parameter ζ can take only a discrete set of values, but this leads to strong restrictions on the field configuration. In particular, one cannot always model an exterior dipole field. Therefore, although this approach is mathematically consistent everywhere, it has the drawback that it does not naturally produce realistic external magnetic field configurations.

The matching conditions we impose at the boundaries are different, and should be considered as an attempt to better approximate realistic boundary conditions. Let us see why. We remind that outside the star we assume there is vacuum and $\zeta = 0$. By comparing (70) and (77) we see that if we choose a_1, a_1' to be continuous across the stellar surface then B_r, B_θ are continuous. However, if $\zeta \neq 0$ inside the star, B_ϕ is discontinuous because, having set $\zeta = 0$ outside, it vanishes there. Such discontinuity corresponds to a surface current

$$
J_\mu^{\text{surf}} = \left(0, 0, -\zeta \frac{e^{-(\lambda+\nu)/2}}{4\pi} a_1 \sin\theta \delta(r - R), 0 \right). \tag{78}
$$

A true neutron star is surrounded by a magnetosphere, where fluid energy density and pressure are small, but currents do not vanish. There, the magnetic field has both poloidal and toroidal components, and both match continuously across the stellar surface with their interior correspondent. The values of a_1, a_1' which would ensure the continuity of both components, would be different from those we choose by imposing $B_\phi = 0$ outside the star; however, with our choice at least we allow the poloidal field, which extends all over the space and decays as r^{-l-2}, to be continuous, whereas outside the star we switch off the toroidal component which extends only in the magnetosphere and tends to zero smoothly at its edges.

A fully consistent magnetar model will need to include a special treatment of the surface (a sort of boundary layer) and presumably also the magnetosphere. In both regions ideal MHD is expected to break down. However, for the present purposes the explicit nature of these regions is probably not important.

The function $a_1(r)$, solution of equation (67), which describes the vector potential inside the star, can have zeros at some points $r = \bar{r}_i$; conversely, the exterior, vacuum solution (76) never vanishes. This happens also in the Newtonian limit; for example, in Perez-Azorin et al. (2006) it has been shown that the solution of the equation corresponding to equation (67) with $c_0 = 0$ is a linear combination of

the spherical Bessel functions

$$j_1(x) = \frac{\sin x}{x^2} - \frac{\cos x}{x},$$
$$n_1(x) = -\frac{\cos x}{x^2} - \frac{\sin x}{x}, \tag{79}$$

where $x = \zeta r$. Such combination vanishes at given values of x. In this case ζ, which has the dimensions of an inverse length, can be interpreted as a sort of wavenumber of the solution.

In our case also, though we set $c_0 \neq 0$, the location of the points where $a_1(r)$ vanishes depend on ζ. If $r = \bar{r} < R$ is a zero of a_1, then $B_r(\bar{r}) = 0$ (see equation 70), and the magnetic flux is confined within the spherical surface $r = \bar{r}$. This means that the field lines inside the star are defined in disjoint domains. Although we do not have a physical interpretation for this configuration, in our study we will not exclude this possibility.

2.5 The ellipticity of the star

The stellar deformation, which we determine by solving the perturbed Einstein equations given in Appendix A, can be expressed in terms of the stellar ellipticity. In the current literature there are two different definitions of ellipticity, which correspond to two conceptually different quantities. The *surface ellipticity*, e_{surf}, is (Chandrasekhar & Miller 1974; Konno et al. 1999, 2000)

$$e_{\mathrm{surf}} = \frac{(\text{equatorial radius}) - (\text{polar radius})}{(\text{polar radius})}. \tag{80}$$

It describes the geometrical shape of the star. It should be mentioned that a slightly different definition has been employed in Hartle (1967), Hartle & Thorne (1968), Benhar et al. (2005), i.e. $\tilde{e}_{\mathrm{surf}} = \sqrt{(e_{\mathrm{surf}})^2 + 2e_{\mathrm{surf}}}$. The surface ellipticity describes the external appearance of the star.

A different quantity is the *quadrupole ellipticity*, e_Q, which is a measure of the mass quadrupole of the star (Bonazzola & Gourgoulhon 1996; Cutler 2002; Haskell et al. 2007):

$$e_Q = -\frac{Q}{I}, \tag{81}$$

where I is the mean value of the moment of inertia of the star I_{ij}, and Q is its mass–energy quadrupole moment. For a stationary, axisymmetric compact object, Q can be extracted by the far field limit of the metric (Hartle & Thorne 1968; Thorne 1980). Indeed, it is the coefficient of the $1/r^3 P_2(\cos\theta)$ term in the expansion of g_{00} in powers of $1/r$ and in Legendre polynomials $P_l(\theta)$:

$$g_{00} \to \cdots - 2Q\frac{1}{r^3}P_2(\cos\theta). \tag{82}$$

As discussed in Thorne (1980) and Laarakkers & Poisson (1999), in the weak field limit the mass–energy quadrupole moment reduces to

$$Q = \int_V \rho(r, \theta) r^2 P_2(\cos\theta) \mathrm{d}V, \tag{83}$$

where V is the star volume. In this limit, the quadrupole tensor of the axially symmetric star can be expressed in terms of Q: $Q_{ij} = \mathrm{diag}(-Q/3, -Q/3, 2/3\,Q)$, and the quadrupole ellipticity can also be written in terms of the inertia tensor

$$e_Q = \frac{I_{zz} - I_{yy}}{I_{zz}}. \tag{84}$$

In the general case, the quadrupole ellipticity is a measure of the entire stellar bulk deformation.

Since e_Q and e_{surf} are quantities with different physical meaning, they are in general different. They coincide only in the case of a constant-density star, in the Newtonian limit, as shown in chapter 16 of Shapiro & Teukolsky (1983).

It is worth stressing that the quadrupole ellipticity is the quantity that should be used to evaluate the gravitational emission of a rotating star; moreover, it has been used to study the spin-flip mechanism proposed by Jones and Cutler (Jones 1975; Cutler 2002).

3 RESULTS

In this section we present the results of the numerical integration of equations (67), (A6) and (A5).

As a test, we have first run our codes for the polytropic star used in Ioka & Sasaki (2004), endowed with mixed (poloidal and toroidal) magnetic field, which vanishes outside the star. Thus, we impose $a_1 = 0$ on the stellar surface $r = R$, and solve the eigenvalue problem to find the set of values ζ_i for which this condition is satisfied. We have reproduced the values of ζ_i given in table 1 of Ioka & Sasaki (2004) for different values of the stellar compactness, with an accuracy better than 1 per cent. The corresponding magnetic field profiles and stellar deformations (surface ellipticity and mass–energy quadrupole) are also in full agreement with (Ioka & Sasaki 2004).

Furthermore, we have integrated the equations for the models considered in Bonazzola & Gourgoulhon (1996); there, non-rotating, magnetized stars with only poloidal fields have been modelled by solving numerically the full set of non-linear Einstein equations; magnetic fields are either defined throughout the star, or confined in the crust. Following (Bonazzola & Gourgoulhon 1996), we introduce the magnetic distortion factor β, given by

$$e_Q = \beta\frac{\mathcal{M}^2}{\mathcal{M}_0^2}, \tag{85}$$

where $\mathcal{M}$ is the magnetic dipole moment, related to magnetic field at the pole, B_{pol}, by

$$\mathcal{M} \equiv B_{\mathrm{pole}} R^3 \frac{4\pi}{2\mu_0}. \tag{86}$$

Here, μ_0 is the magnetic permeability. The normalization factor $\mathcal{M}_0$ is given by

$$\mathcal{M}_0 \equiv \frac{4\pi}{\mu_0}\frac{G I^2}{R^2}. \tag{87}$$

With this normalization, the coefficient β is dimensionless. Moreover, as $e_Q = O(B^2)$ and $\mathcal{M} = O(B)$, β is nearly independent of B, and indicates to what extent a star can be deformed by the magnetic field. It is worth mentioning that the magnetic dipole $\mathcal{M}$ defined in (86) differs from the quantity μ defined in equation (76), since equation (86) has been derived in the context of Newtonian theory. As in Bonazzola & Gourgoulhon (1996), we use the EOS of Wiringa, Fiks & Fabrocini (1988), and consider an $M = 1.4\,\mathrm{M}_\odot$ star.

When the magnetic field extends throughout the star, we find $\beta = 0.505$, while the authors of (Bonazzola & Gourgoulhon 1996) find $\beta = 1.01$; when the field is confined to the crust, we find $\beta \sim 5$, while the authors of (Bonazzola & Gourgoulhon 1996) find a very large value: $\beta \sim 10^2$. However, if we compute β from the same equation, but using e_{surf} instead of e_Q, we find $\beta = 1.01$ when the magnetic field extends throughout the star, and $\beta \sim 10^2$ in the case of crustal fields, in agreement with (Bonazzola & Gourgoulhon 1996).

The reason why, when crustal fields are present, the factor β computed using e_{surf} is much larger than that computed using e_Q,

is the following. The crust contains a very small fraction of stellar matter therefore, although its deformation is large (because the field lines are squeezed in a small region), it does not induce a big change in the distribution of matter in the stellar bulk. As a consequence, $e_{\mathrm{surf}} \gg e_{\mathrm{Q}}$.

3.1 Deformations induced by different magnetic field configurations

We shall now study how the stellar deformations induced by a mixed (poloidal and toroidal) magnetic field depend on the field configuration. To describe matter in the stellar core we use the EOS of Akmal, Pandharipande & Ravenhall (1998) (denoted as APR2); we choose a star with mass $M = 1.4\,\mathrm{M}_\odot$ and a radius $R = 11.58$ km. The magnetic field is normalized assuming that its value at the pole is $B_{\mathrm{pole}} = 10^{15}$ G. For the different configurations discussed in Section 2.4, we find the magnetic field structure, the surface and quadrupole ellipticities $e_{\mathrm{surf}}, e_{\mathrm{Q}}$, and the maximal values of the internal poloidal and toroidal fields, $B_{\mathrm{p}}^{\mathrm{max}}$ and $B_{\mathrm{t}}^{\mathrm{max}}$. The equations for the stellar deformation and the procedure to compute $e_{\mathrm{surf}}, e_{\mathrm{Q}}$ are described in Appendix A.

We stress that it is important to determine if the magnetic star has a an oblate or prolate shape, i.e. to determine the sign of e_{Q}; indeed, as suggested by Jones and Cutler (Jones 1975; Cutler 2002), if $e_{\mathrm{Q}} < 0$ the star could change its rotation axis due to viscous forces ('spin flip') becoming an orthogonal rotator (with magnetic axis orthogonal to the rotation axis), and the process could be associated to a large gravitational wave emission. In this respect, it is also important to determine the absolute values of the allowed quadrupole ellipticities, because if the star rotates around an axis different from the magnetic field symmetry axis, it emits gravitational waves with

amplitude (Bonazzola & Gourgoulhon 1996)

$$h_0 \sim \frac{4G}{rc^4}\Omega^2 I |e_{\mathrm{Q}}|, \tag{88}$$

and frequency $\nu_{\mathrm{GW}} = \Omega/(2\pi)$, where Ω is the angular velocity.

It is worth stressing that the current upper bound on neutron star ellipticity, i.e. $|e_{\mathrm{Q}}| \lesssim 10^{-6}$, is obtained by evaluating the maximal strain that the crust of an old and cold neutron star can sustain (Ushomirsky, Cutler & Bildsten 2000; Haskell, Jones & Andersson 2006). However, a large deformation may be induced by the effect of strong magnetic fields in the very early phases of the stellar life, when the crust has not formed yet. These deformation may persist as the star cools down, leading to final configurations having an ellipticity larger than the above limit. Let us now discuss the two field configurations described in Section 2.4.

3.1.1 Magnetic field defined throughout the star

If the magnetic field is non-vanishing through the whole star (see Section 2.4), we find that $a_1(r)$ has no nodes for $r < R$ in two ranges:

range 1 : $(0 \leqslant \zeta \leqslant 0.2915)$,

range 2 : $(0.369 \leqslant \zeta \leqslant 0.46)$. $\tag{89}$

If ζ lies outside these ranges, the field lines inside the star are defined in disjoint domains, as discussed in Section 2.4.

In Fig. 1 we plot the magnetic field components versus the radial distance, for $r \leqslant R$. $B_{(r)}$ is evaluated at $\theta = 0$, $B_{(\theta)}$ and $B_{(\phi)}$ are evaluated at $\theta = \pi/2$. The plots are shown for four values of ζ (in km^{-1}): $\zeta = 0.15$ in Fig. 1(a); this value is in the range 1, $\zeta = 0.37$ in Fig. 1(b), $\zeta = 0.4$ in Fig. 1(c); both values are in the range 2 and $\zeta = 0.3$ in Fig. 1(d), which is outside the ranges 1 and 2.
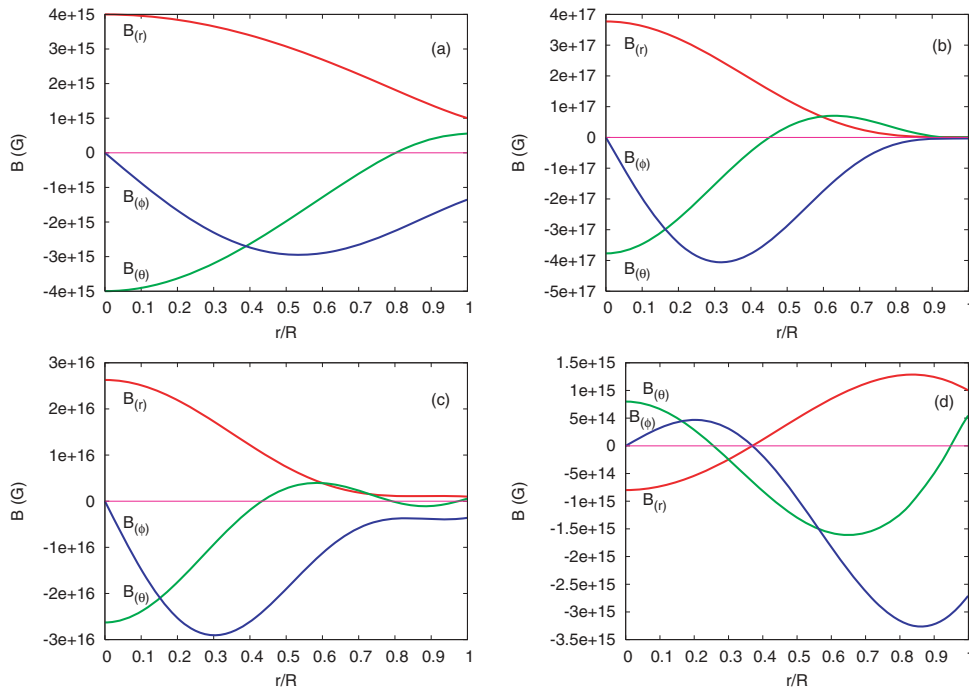

Figure 1. The profiles of $B_{(r)}$ evaluated at $\theta = 0$, and of $B_{(\theta)}$ and $B_{(\phi)}$, evaluated at $\theta = \pi/2$, are plotted as functions of the normalized radius inside the star. The magnetic field is defined through the whole star. Each panel corresponds to a value of ζ: $\zeta = 0.15$ km^{-1} in panel (a), $\zeta = 0.37$ km^{-1} in (b), $\zeta = 0.40$ km^{-1} in (c) and $\zeta = 0.30$ km^{-1} in (d). Panel (d) refers to a value of ζ exterior to the ranges (89); thus in this case the magnetic field lines are defined in disjoint domains (see text).
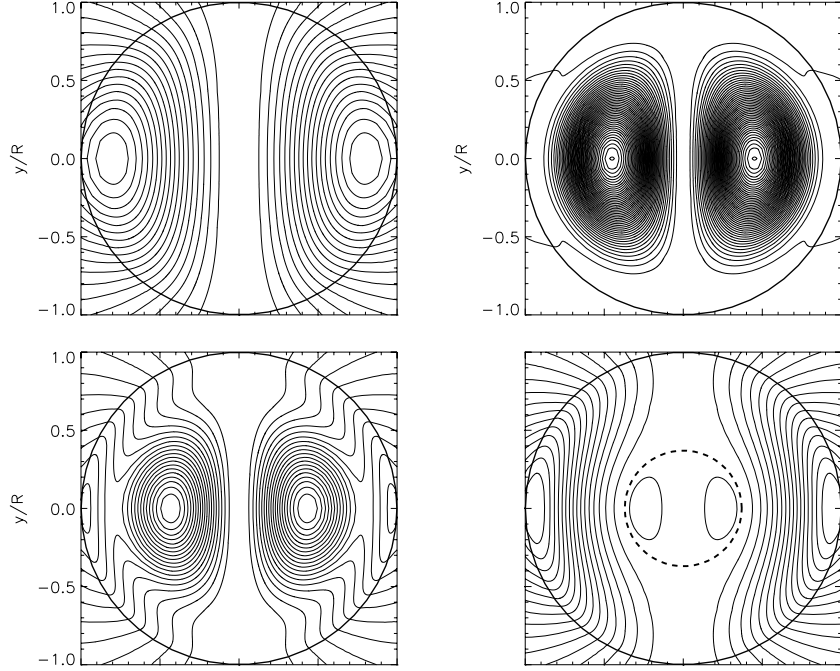
Figure 2. The projection of the field lines in the meridional plane is shown for $\zeta = 0.15\,\text{km}^{-1}$ (upper panel, left-hand side), $\zeta = 0.37\,\text{km}^{-1}$ (upper panel, right), $\zeta = 0.40\,\text{km}^{-1}$ (lower panel, left-hand side) and $\zeta = 0.30\,\text{km}^{-1}$ (lower panel, right-hand side). The dashed circle in the lower panel on the right-hand side separates two disjoint domains. The magnetic field extends throughout the star.

Different values of ζ give qualitatively similar behaviours. We see that when ζ approaches the lower bound of range 2, as in Fig. 1(b), the field components become much larger than in the other cases. Of course they cannot be arbitrarily large, since they must not exceed the virial theorem limit $B \lesssim 10^{18}$ G (Boquet et al. 1995). This is a peculiar behaviour, which is not observed if one approaches the other bounds of range 1 and 2, either from inside or from outside. The reason for such behaviour is that the configuration with $\zeta = 0.369\,\text{km}^{-1}$ is a singular limit. It corresponds to a configuration in which $a_1(R) = 0$, i.e. the magnetic field is confined inside the star and vanishes outside. This is inconsistent with the boundary condition we impose, i.e. $B_{\text{pole}} = 10^{15}$ G. Thus, this singular value is unacceptable. However, values of ζ approaching this limit can be accepted, provided the virial limit is not violated. We mention that, as long as B is smaller than the virial limit, the stress–energy tensor of the electromagnetic field is smaller than that of the fluid, and the perturbative approach we use is appropriate.

The field profiles shown in Fig. 1(d) refer to a case in which inside the star the field lines are defined in disjoint domains: indeed, they cannot cross the sphere $r = 0.37;R$ since $B_r(r = 0.37R) = 0$.

The projection of the field lines in the meridional plane is shown in Fig. 2; the four panels refer to the same values of ζ considered in Fig. 1. Fig. 2(d) corresponds to $\zeta = 0.3$, i.e. to the case of disjoint domains: field lines do not cross the dashed circle in the picture.

The ellipticities e_{surf} and e_Q are plotted in Fig. 3 as functions of $\zeta \in [0, 0.5]$. Continuous lines correspond to values of ζ inside the ranges (89) (no nodes inside the star), while the dashed lines correspond to values of ζ for which there is a node inside the star.

For small values of ζ (i.e. if the poloidal field prevails) the star is oblate ($e_{\text{surf},Q} > 0$). As ζ increases, the toroidal part becomes more important and the star becomes prolate ($e_{\text{surf},Q} < 0$). In other words, the toroidal field tends to make the star prolate, while the poloidal field tends to make it oblate; this behaviour has already
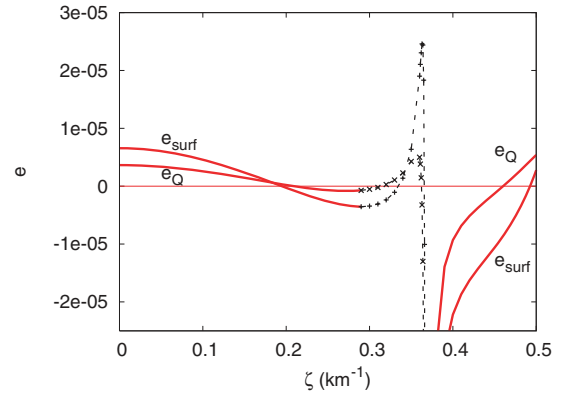

Figure 3. Surface and quadrupole ellipticities as functions of ζ for a star with mass $M = 1.4\,\text{M}_\odot$, and EOS APR2. The magnetic field extends throughout the star. The dashed (solid) lines correspond to models for which $a_1(r)$ has nodes (has no nodes) inside the star.

been discussed in the literature, see for instance (Ioka & Sasaki 2004). For larger values of ζ the behaviour is different. If we exclude values close to the singular point $\zeta \simeq 0.369\,\text{km}^{-1}$, we find that the ellipticity is

$$|e_{\text{surf},Q}| \simeq 10^{-6}\text{–}10^{-5}. \tag{90}$$

If we approach the value $\zeta = 0.369$ from either sides, then $e_{\text{surf},Q} < 0$, and the deformation can be much larger; the virial theorem constraint, $B \lesssim 10^{18}$ G, corresponds to

$$|e_{\text{surf}}| \lesssim 2 \times 10^{-3} \;, \quad |e_Q| \lesssim 10^{-3}. \tag{91}$$

Thus, for a large range of values of ζ, the magnetic field induces a shape, either prolate or oblate, with $|e_Q| \sim 10^{-6}$ to 10^{-5}; however,

Table 1. Surface and quadrupole ellipticities and maximal values of the internal poloidal and toroidal magnetic fields are tabulated for different values of ζ.

ζ (km^{-1})	e_{surf}	e_Q	$B^p_{\max}/(10^{15}\,\text{G})$	$B^t_{\max}/(10^{15}\,\text{G})$
0	6.572×10^{-6}	3.642×10^{-6}	4.579	0
0.05	6.057×10^{-6}	3.364×10^{-6}	4.522	1.112
0.1	4.580×10^{-6}	2.582×10^{-6}	4.341	2.132
0.15	2.349×10^{-6}	1.447×10^{-6}	3.998	2.948
0.2	-2.661×10^{-7}	2.199×10^{-7}	3.391	3.404
0.25	-2.643×10^{-6}	-6.945×10^{-7}	2.219	3.303
0.30	-3.433×10^{-6}	-5.343×10^{-7}	1.610	3.264
0.37	-1.106×10^{-3}	-2.250×10^{-3}	518.0	557.0
0.35	6.375×10^{-6}	4.273×10^{-6}	21.52	22.15
0.40	-2.220×10^{-5}	-9.313×10^{-6}	26.28	29.05
0.45	-1.062×10^{-5}	-1.263×10^{-6}	18.89	20.51
0.50	2.773×10^{-6}	5.410×10^{-6}	26.68	27.50

for very particular values of ζ, the star can have a strongly prolate shape ($e_Q < 0$), with $|e_Q|$ as large as 10^{-3}.

In Table 1 we give, for selected values of ζ in the range [0, 0.5] km^{-1}, the surface and quadrupole ellipticities, and the maximal values of the internal poloidal and toroidal fields. It is interesting to note that for values of $\zeta \lesssim 0.1$, $e_{\text{surf}} \simeq 2e_Q$. We find a similar behaviour when the ellipticity is induced by rotation and no magnetic field is present. Indeed, by integrating the equations of stellar deformation to second order in the angular velocity as in Benhar et al. (2005), we find that, for a large variety of neutron star EOSs, $e_{\text{surf}} \simeq 2e_Q$ for $\Omega \lesssim 0.1\,\Omega_{\text{ms}}$, where $\Omega_{\text{ms}} = \sqrt{M/R^3}$.

3.1.2 Crustal fields

When the magnetic field is confined to the crust, we find that $a_1(r)$ has no nodes inside the star for

$$0 \leqslant \zeta \leqslant 1.085. \qquad (92)$$

$a_1(R) \neq 0$ for all values of ζ, therefore crustal field do not exhibit the singular behaviour discussed in Section 3.1.1.

In the upper panel of Fig. 4 we show, for $r \leqslant R$, the profiles of $B_{(r)}$ evaluated at $\theta = 0$, and of $B_{(\theta)}$ and $B_{(\phi)}$ evaluated at $\theta = \pi/2$, for $\zeta = 0.5$ km^{-1}. Different values of ζ correspond to qualitatively similar behaviours. We see that the interior field is one order of magnitude larger than the surface field; this behaviour, peculiar of crustal fields, is common to all values of ζ. The projection of the field lines in the meridional plane is shown in the lower panel.

In Fig. 5 we show the ellipticities as functions of ζ; continuous lines correspond to values of ζ inside the range (92), dashed lines to values outside that range. We see that, as discussed in the previous section, the geometrical shape of the star is oblate for small values of ζ (for which $e_{\text{surf}} > 0$) and prolate for larger values: the surface ellipticity is a monotonically decreasing function of ζ. Conversely, the quadrupole ellipticity is always positive and, in modulus, much smaller than e_{surf}, even for values of ζ larger than those considered in Fig. 5. We note that these results rule out the Jones–Cutler mechanism in the case of crustal fields, since it can only occur when $e_Q < 0$. As explained in Section 3, the reason why $e_{\text{surf}} \gg e_Q$ is that, though the crust deformation is large since the field lines are squeezed in a small region, it does not induce a big change in the distribution of matter in the stellar bulk.

In Table 2 we give, for selected values of ζ in the range [0, 1.5] km^{-1}, the surface and quadrupole ellipticities, and the maximal values of the internal poloidal and toroidal fields. Comparing
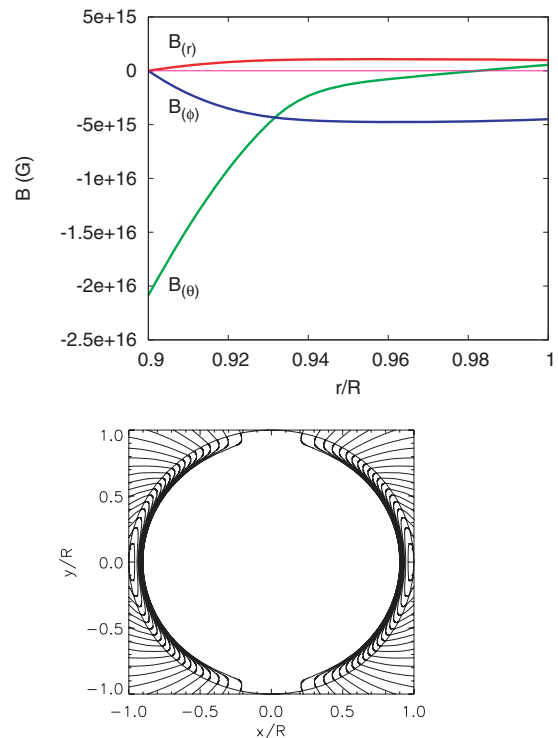

Figure 4. The profiles of $B_{(r)}$, evaluated at $\theta = 0$, and of $B_{(\theta)}$ and $B_{(\phi)}$ evaluated at $\theta = \pi/2$, are plotted for $\zeta = 0.5$ km^{-1} in the crust (upper panel). The projection of the field lines in the meridional plane is shown in the lower panel, for the same value of ζ.

Tables 1 and 2 we see that, for crustal fields, typical values of e_{surf} are two orders of magnitude larger than for fields extending through the whole star. The quadrupole ellipticity is, typically, one order of magnitude larger:

$$|e_{\text{surf}}| \sim 10^{-4} - 10^{-3}, \quad e_Q \sim 10^{-5} - 10^{-4}, \qquad (93)$$

with the exception of the models with ζ close to 0.369, for which the deformation is larger in the case of fields extending throughout the star.
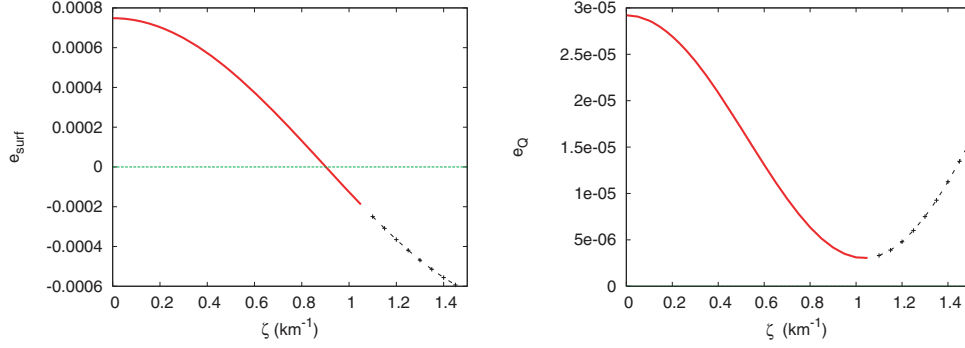
Figure 5. The surface (left-hand panel) and quadrupole (right-hand panel) ellipticities are plotted as functions of ζ for a star with mass $M = 1.4\,\mathrm{M}_\odot$ and EOS APR2, when the magnetic field is confined to the crust. The dashed (solid) lines correspond to models for which $a_1(r)$ has nodes (has no nodes) inside the star.

Table 2. Surface and quadrupole ellipticities and maximal values of the internal poloidal and toroidal magnetic fields are given for different values of ζ in the case of crustal fields.

ζ (km^{-1})	e_{surf}	e_{Q}	$B^p_{\max}/(10^{15}\,\mathrm{G})$	$B^t_{\max}/(10^{15}\,\mathrm{G})$
0	7.483×10^{-4}	2.921×10^{-5}	27.80	0
0.2	7.031×10^{-4}	2.693×10^{-5}	26.65	2.081
0.4	5.731×10^{-4}	2.086×10^{-5}	23.29	3.924
0.6	3.744×10^{-4}	1.310×10^{-5}	18.00	5.616
0.8	1.313×10^{-4}	6.352×10^{-6}	11.19	7.361
1.0	-1.259×10^{-4}	3.113×10^{-6}	6.580	9.130
1.2	-3.653×10^{-4}	4.798×10^{-6}	8.216	10.91
1.4	-5.564×10^{-4}	1.127×10^{-5}	12.30	12.70
1.5	-6.257×10^{-4}	1.581×10^{-5}	15.79	13.59

3.2 Comparison between magnetic and rotational deformations

Both rotation and magnetic field contribute to the ellipticity of the star, i.e. $e_{\mathrm{surf,Q}} = e^{\Omega}_{\mathrm{surf,Q}} + e^B_{\mathrm{surf,Q}}$. It is interesting to compare the two contributions, evaluated in the range of parameters typical of observed magnetars (SGR and AXP), i.e. (Woods & Thompson 2006)

$$0.6 \times 10^{14} \lesssim B \lesssim 7.8 \times 10^{14}\,\mathrm{G}, \tag{94}$$

$$5.2 \lesssim T \lesssim 11.8\,\mathrm{s}, \tag{95}$$

where T is the rotational period. It should be mentioned that, as explained in Cutler (2002), only e^B_{Q} contributes to the spin-flip process, which occurs when $e^B_{\mathrm{Q}} < 0$.

We have computed $e^{\Omega}_{\mathrm{surf,Q}}$ for an $M = 1.4\,\mathrm{M}_\odot$ star with EOS APR2, using the codes, developed by some of us (Benhar et al. 2005), which describe the structure of a non-magnetized, rotating star, up to $O(\Omega^3)$; $e^B_{\mathrm{surf,Q}}$ have been computed using the approach described in this paper.

In Fig. 6 we show $|e_{\mathrm{surf}}|$ and $|e_{\mathrm{Q}}|$ as functions of ζ, for the two magnetic field configurations described in Section 2.4: field throughout the star (upper panels), and crustal fields (lower panels). The two solid lines correspond the $|e^B_{\mathrm{surf,Q}}|$ computed for B_{pole} equal to the minimum and maximum values of the range (94). The shadowed region corresponds to the rotation contribution, $e^{\Omega}_{\mathrm{surf,Q}}$, for rotation periods in the range (95). The dashed lines correspond to $T = 1$ and 0.1 s, outside that range and smaller than the observed periods of SGRs and AXPs: we show these values since they may possibly occur in young magnetars. From Fig. 6 we see that for the observed

magnetars $|e^B_{\mathrm{Q,surf}}|$ is typically larger than $|e^{\Omega}_{\mathrm{Q,surf}}|$. This behaviour is magnified when crustal field are present (lower panels in Fig. 6). The rotational contribution may significantly exceed that of magnetic field only for stars rotating faster (dashed lines). The solid line minima in the pictures correspond to the points where $e^B_{\mathrm{Q,surf}} = 0$; there the effects of the poloidal and toroidal fields balance and the ellipticity changes sign.

3.3 Deformation of magnetized stars with different masses and EOS

The results discussed in previous sections where obtained for a star with mass $M = 1.4\,\mathrm{M}_\odot$ and EOS APR2. We shall now see how the results depend on the EOS and on the stellar mass. To this purpose, as an example we shall consider three different EOSs:

(i) APR2 (Akmal et al. 1998), derived within the non-relativistic nuclear many-body theory, assuming that the star is made of ordinary nuclear matter; the maximum mass is $M_{\max} = 2.202\,\mathrm{M}_\odot$.

(ii) G240 (Glendenning 2000), derived within the relativistic mean-field theory and allowing for the presence of hyperons in coexistence with ordinary nuclear matter; $M_{\max} = 1.553\,\mathrm{M}_\odot$.

(iii) QS, based on the MIT bag model (Chodos et al. 1974) (with $B = 95\,\mathrm{MeV\,fm}^{-3}, \alpha_s = 0.4, m_s = 100\,\mathrm{MeV}$), assuming that the star is a bare quark star, i.e. composed entirely of deconfined quark matter; $M_{\max} = 1.445\,\mathrm{M}_\odot$.

G240 with hyperons is a very soft EOS, QS is very stiff (for a comparative discussion of these EOSs see Benhar et al. 2004, 2005). Furthermore we shall consider the two magnetic field
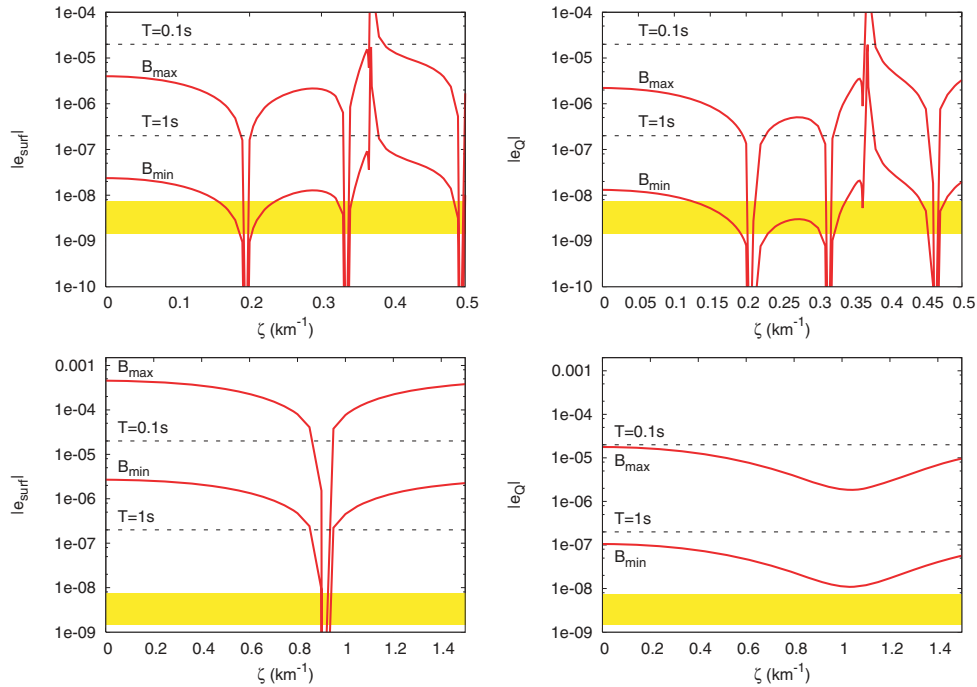
Figure 6. $|e_{surf}|$ and $|e_Q|$ are plotted as functions of ζ, for two magnetic field configurations: field throughout the star (upper panels), and crustal fields (lower panels). The two solid lines refer to $|e_{surf,Q}^B|$ computed for $B_{pole} = B_{min,max}$ corresponding to the extrema of the range (94). The shadowed region corresponds to $e_{surf,Q}^\Omega$ evaluated for rotation periods in the range (95). The dashed lines correspond to rotation periods of $T = 0.1$ and 1 s.

configurations discussed in Section 2.4, and two values of mass, $M = 1.2$ and $1.4\,M_\odot$.

In Fig. 7 we show e_{surf} and e_Q as functions of ζ, for $M = 1.2\,M_\odot$ (upper panels) and for $M = 1.4\,M_\odot$ (lower panels), for the selected EOS, when the magnetic field extends throughout the star. We see

that, as expected, softer EOS and smaller mass correspond to larger deformations. For all masses and EOS, we find the same qualitative behaviour shown in Fig. 3.

In Fig. 8, e_{surf} and e_Q are shown in the case of crustal fields. We find that e_{surf} depends strongly on the mass and the EOS. For an
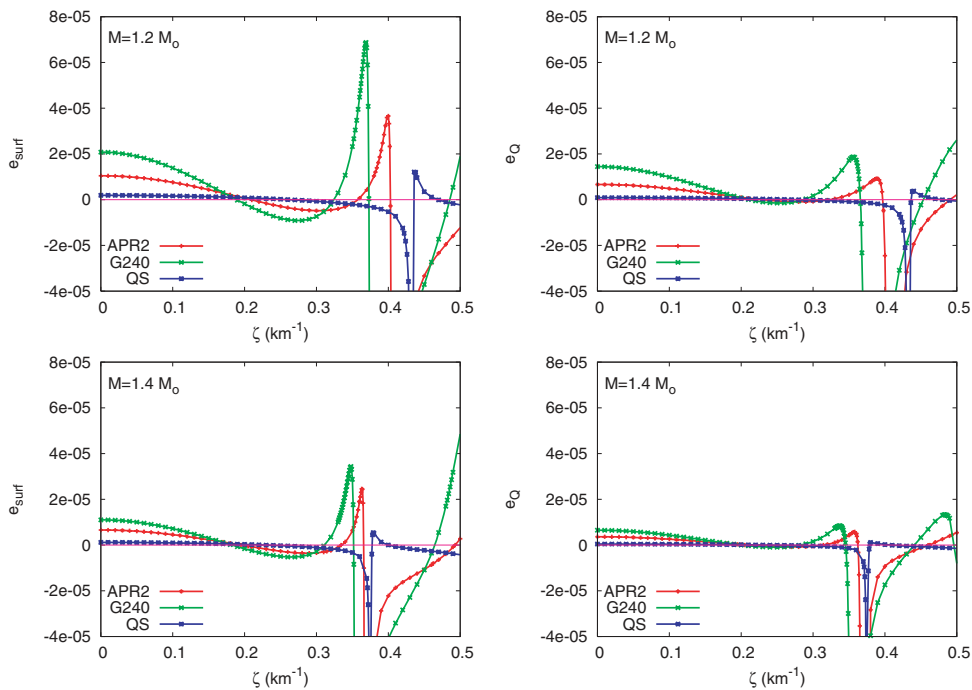

Figure 7. Surface and quadrupole ellipticities as functions of ζ for different EOSs and magnetic fields extending throughout the star. The stellar mass is $M = 1.20\,M_\odot$ (upper panels) and $M = 1.40\,M_\odot$ (lower panels).
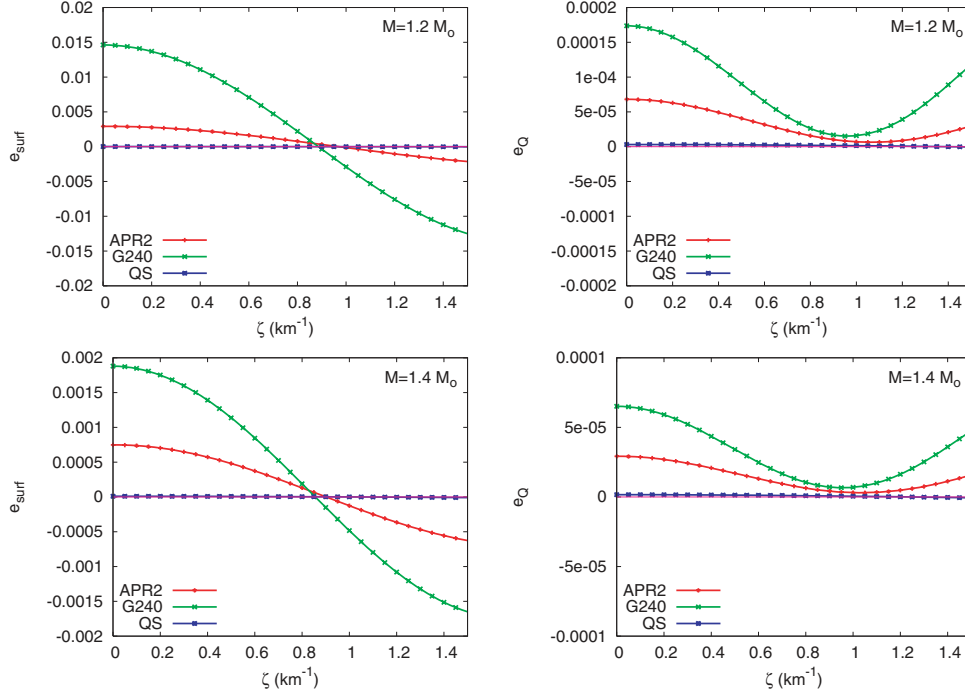
Figure 8. Surface and quadrupole ellipticities are plotted as in Fig. 7 in the case of crustal fields.

assigned EOS, changing the mass from 1.4 to 1.2 $M_\odot$, e_{surf} increases by a factor of ~ 10, and e_Q by a factor of ~ 2. If we fix the mass and change the EOS we find

$$e_{\mathrm{surf},Q}(\mathrm{G240})/e_{\mathrm{surf},Q}(\mathrm{APR2}) \sim [2\text{--}4],$$

whereas

$$e_{\mathrm{surf},Q}(\mathrm{APR2})/e_{\mathrm{surf},Q}(\mathrm{QS}) \sim [10\text{--}100].$$

Finally, we find that for the stiffest EOS we consider (QS), for some values of ζ the quadrupole ellipticity can become negative, whereas this never occurs for APR2 and G240.

It should be stressed that when magnetic fields extend throughout the star the dependence of the ellipticities on the EOS and on the mass is considerably weaker (Fig. 7).

3.4 Higher order multipoles

In this paper we have focused on the study of dipole ($l = 1$) magnetic fields, which decay as r^{-l-2} and therefore dominate far away from the star. In this Section we solve the Grad–Shafranov equation (68) for $l = 2$, including both poloidal and toroidal components:

$$\mathrm{e}^{-\lambda}a_2'' + \frac{\nu' - \lambda'}{2}\mathrm{e}^{-\lambda}a_2' + \left(\zeta^2\mathrm{e}^{-\nu} - \frac{6}{r^2}\right)a_2 = 0. \qquad (96)$$

For fields extending throughout the star, we impose a regular behaviour near the origin: $a_2(r \simeq 0) = \alpha_0 r^3 + O(r^5)$. In the case of crustal fields the regularity condition is imposed near the crust–core interface, i.e. $a_2(r \gtrsim r_c) = \alpha_2(r - r_c) + O((r - r_c)^2)$.

We assume that the field vanishes outside the star, i.e. $a_2(r > R) = 0$. Continuity of a_2 (and then of B_r) on the stellar surface, implies $a_2(R) = 0$; thus we have to solve an eigenvalue

problem (like in Ioka & Sasaki 2004; Haskell et al. 2007), to select the discrete set of values $\zeta = \zeta_i$ for which the boundary conditions are satisfied. The eigenfunction $a_2(r)$, which corresponds to ζ_i, has i nodes, one of which is located at the stellar surface. We note that, since as mentioned in Section 2.3, only the current J^t_μ contributes to a_l when $l > 1$, we do not have as much freedom as in the $l = 1$ case, when we used the constant c_0 to impose $a_2'(R) = 0$; consequently, a_2' is discontinuous (and so is B_θ) on the stellar surface.

For a star with $M = 1.4\,M_\odot$, described by the EOS APR2, we have determined the field configurations corresponding to the first five eigenvalues ζ_i. Since the field vanishes on the stellar surface, we normalize B by choosing α_0 such that the maximum value of the magnetic field inside the star is $B_{\mathrm{max}} = 10^{16}$ G, i.e. of the same order of magnitude of the field considered in Section 3.1 for $l = 1$ (see Tables 1 and 2). Then we have solved the equations of stellar deformation given in Section A2, finding the surface and quadrupole ellipticities.

The projection of the field lines in the meridional plane is shown in Fig. 9 for the first two eigenvalues. The upper panels refer to fields defined throughout the star, the lower panels to crustal fields.

In Tables 3 and 4 we give the first five eigenvalues ζ_i and the corresponding ellipticities, for fields extending throughout the star and for crustal fields, respectively. In the first case the ellipticities are always negative and of the order

$$|e_{\mathrm{surf},Q}| \sim 10^{-7}\text{--}10^{-6}, \qquad (97)$$

i.e. smaller than for the $l = 1$ fields. For crustal fields, ellipticities are always positive and of the same order of magnitude as for $l = 1$, i.e.
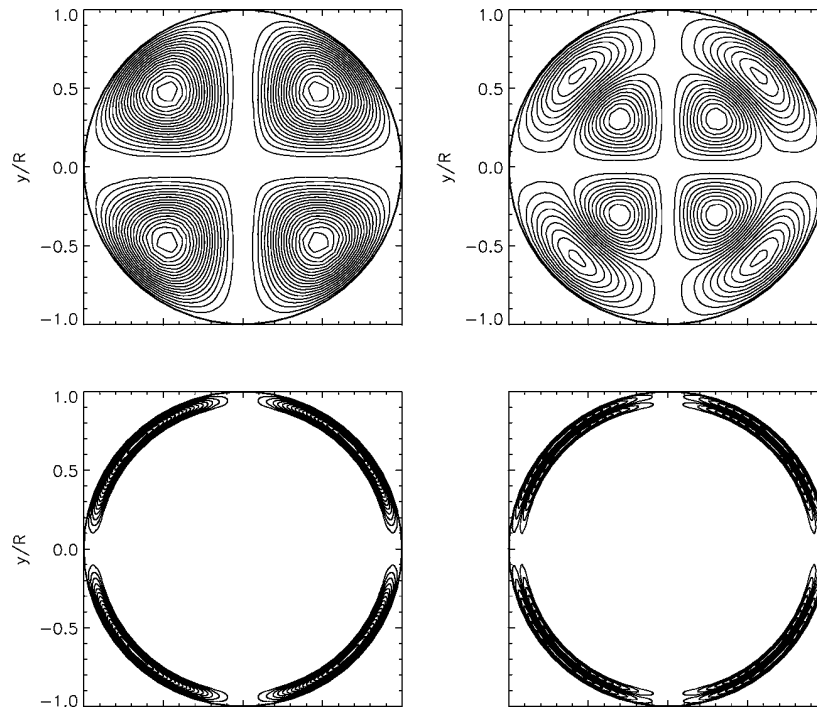
$$e_{\mathrm{surf},Q} \sim 10^{-5}. \qquad (98)$$

Figure 9. The projection of the $l = 2$ field lines in the meridional plane is shown for $\zeta = \zeta_1$ (left-hand panels) and $\zeta = \zeta_2$ (right-hand panels). The upper panels refer to fields extending throughout the star, the lower panels to crustal fields.

Table 3. First eigenvalues ζ_i and the corresponding surface and quadrupole ellipticities for $l = 2$ magnetic fields extending throughout the star.

ζ (km^{-1})	e_{surf}	e_Q
0.325	-5.07×10^{-6}	-6.24×10^{-6}
0.495	-1.78×10^{-6}	-2.19×10^{-6}
0.662	-9.37×10^{-7}	-1.15×10^{-6}
0.829	-5.80×10^{-7}	-7.13×10^{-7}
0.996	-3.95×10^{-7}	-4.85×10^{-7}

Table 4. First eigenvalues ζ_i and the corresponding surface and quadrupole ellipticities for $l = 2$ crustal fields.

ζ (km^{-1})	e_{surf}	e_Q
1.705	1.75×10^{-5}	2.16×10^{-5}
3.397	1.64×10^{-5}	2.01×10^{-5}
5.091	1.60×10^{-5}	1.96×10^{-5}
6.787	1.58×10^{-5}	1.94×10^{-5}
8.482	1.56×10^{-5}	1.92×10^{-5}

4 CONCLUDING REMARKS

In this paper we solve Einstein–Maxwell equations, using a perturbative approach, to study the structure of the magnetic field of magnetars, and to find the deformation it induces on the star. We extend previous works on the subject (Ioka & Sasaki 2004; Konno et al. 1999, 2000; Haskell et al. 2007) in several respects: we include toroidal fields inside the star, thus removing the assumption, used in Boquet et al. (1995), Bonazzola & Gourgoulhon (1996), Cardall et al. (2001), of circular space–time; we determine both the surface ellipticity and the quadrupole ellipticity; we explore various field configurations, corresponding to different boundary conditions; we compare the effects produced by a magnetic field and by rotation on the stellar structure; we study how different EOSs and masses affect the magnetic field structure and the quadrupole ellipticity it induces; we solve the equations for higher order ($l = 2$) multipoles.

In summary, the main results of our study are the following.

(i) Crustal fields induce surface deformations much larger than fields extending throughout the star, but the quadrupole deformations are comparable in the two cases. Typically, crustal fields produce oblate, rather than prolate shapes.

(ii) For particular values of the parameter ζ, representing the ratio between toroidal and poloidal components, the magnetic field inside the star and the deformation can be extremely large; such configurations correspond to prolate shapes.

(iii) For the typical rotation rates of observed magnetars, the deformation induced by rotation is much smaller than that induced by the magnetic field.

(iv) Neutron stars with the same magnetic field, but with softer EOS or smaller mass, exhibit larger deformations.

(v) If the magnetic field extends throughout the star, the deformations induced by higher order ($l = 2$) multipoles are one order of magnitude smaller than the dipolar contributions; for crustal fields, they are comparable.

As a future extension of this work, we plan to study the effect of couplings between different multipoles, which we have neglected in the present paper, and to determine their relative weights. Furthermore, the equilibrium configurations we have found will be used as background models to study the oscillations of highly magnetized neutron stars.

REFERENCES

Akmal A., Pandharipande V. R., Ravenhall D. G., 1998, Phys. Rev. C, 58, 1804

Bekenstein J. D., Oron E., 1978, Phys. Rev. D, 18, 1809

Bekenstein J. D., Oron E., 1979, Phys. Rev. D, 19, 2827

Benhar O., Ferrari V., Gualtieri L., 2004, Phys. Rev. D, 70, 124015

Benhar O., Ferrari V., Gualtieri L., Marassi S., 2005, Phys. Rev. D, 72, 044028

Bonanno A., Rezzolla L., 2003, A&A, 410, L33

Bonazzola S., Gourgoulhon E., 1996, A&A, 312, 675

Bonazzola S., Gourgoulhon E., Salgado M., Marck J. A., 1993, A&A, 278, 421

Boquet M., Bonazzola S., Gourgoulhon E., Novak J., 1995, A&A, 301, 757

Braithwaite J., Spruit H. C., 2006, A&A, 450, 1097

Cardall C. Y., Prakash M., Lattimer L. M., 2001, ApJ, 554, 322

Carter B., 1973, in DeWitt C., DeWitt B. S., eds, Black Holes – Les Houches 1972. Gordon & Breach Science Publishers, New York

Chandrasekhar S., Miller J. C., 1974, MNRAS, 167, 63

Chodos A., Jaffe R. L., Johnson K., Thorne C. B., Weiskopf V. F., 1974, Phys. Rev. D, 9, 3471

Cutler C., 2002, Phys. Rev. D, 66, 084025

Duncan R. C., Thompson C., 1992, ApJ, 392, L9

Flowers E., Ruderman M., 1977, ApJ, 215, 302

Glendenning N. K., 2000, Compact Stars. Springer-Verlag, New York

Hartle J. B., 1967, ApJ, 150, 1005

Hartle J. B., Thorne K. S., 1968, ApJ, 153, 807

Haskell B., Jones D. I., Andersson N., 2006, MNRAS, 373, 1423

Haskell B., Samuelsson L., Glampedakis K., Andersson N., 2007, preprint (arXiv:0705.1780)

Ioka K., Sasaki M., 2003, Phys. Rev. D, 67, 124026

Ioka K., Sasaki M., 2004, ApJ, 600, 296

Israel G. L. et al., 2005, ApJ, 628, L53

Jones P. B., 1975, Ap&SS, 33, 215

Kluzniak W., Ruderman M., 1998, ApJ, 505, L113

Konno K., Obata T., Kojima Y., 1999, A&A, 352, 211

Konno K., Obata T., Kojima Y., 2000, A&A, 356, 234

Kouveliotou C., Dieter S., Strohmayer T., van Paradijs J., Fishman G. J., Meegan C. A., Hurley K., 1998, Nat, 393, 235

Laarakkers W. G., Poisson E., 1999, ApJ, 512, 282

Mereghetti S., Stella L., 1995, ApJ, 442, L17

Oron A., 2002, Phys. Rev. D, 66, 023006

Perez-Azorin J. F., Miralles J. A., Pons J. A., 2006, A&A, 451, 1009

Pons J. A., Geppert U., 2007, A&A, 470, 303

Samuelsson L., Andersson N., 2005, MNRAS, 374, 256

Shapiro S. L., Teukolsky S. A., 1983, Black Holes, White Dwarfs and Neutron Stars. Wiley, New York

Sotani H., Kokkotas K. D., Stergioulas N., 2007, MNRAS, 375, 261

Strohmayer T. E., Watts A. L., 2005, ApJ, 632, L111

Thompson C., Duncan R. C., 1993, ApJ, 408, 194

Thorne K. S., 1980, Rev. Mod. Phys., 52, 299

Ushomirsky G., Cutler C., Bildsten L., 2000, MNRAS, 319, 902

Usov V. V., 1992, Nat, 357, 472

Wheeler J. C., Yi I., Höflich P., Wang L., 2000, ApJ, 537, 810

Wiringa R. B., Fiks V., Fabrocini A., 1988, Phys. Rev. C, 38, 1010

Woods P. M., Thompson C., 2006, in Lewin W., van der Kils M., eds, Cambridge Astrophysics Series Vol. 39, Compact Stellar X-ray Sources. Cambridge Univ. Press, Cambridge, p. 547

Yoshida S., Eriguchi Y., 2006, ApJ, 164, 156

Yoshida S., Yoshida S., Eriguchi Y., 2006, ApJ, 651, 462

APPENDIX A: THE DEFORMATIONS OF THE STAR

The metric of a non-rotating star deformed by a magnetic field can be written, up to $O(B^2)$, as (Ioka & Sasaki 2004)

$$
\begin{aligned}
ds^2 = {} & -e^\nu \left(1 + 2[h_0 + h_2 P_2(\cos\theta)]\right) dt^2 \\
& + e^\lambda \left(1 + \frac{2e^\lambda}{r}[m_0 + m_2 P_2(\cos\theta)]\right) dr^2 \\
& + r^2[1 + 2k_2 P_2(\cos\theta)](d\theta^2 + \sin^2\theta\, d\phi^2) \\
& + 2\left[i_1 P_1(\cos\theta) + i_2 P_2(\cos\theta) + i_3 P_3(\cos\theta)\right] dt\, dr \\
& + 2\sin\theta \left[v_1 \frac{\partial}{\partial\theta} P_1(\cos\theta) + v_2 \frac{\partial}{\partial\theta} P_2(\cos\theta) \right. \\
& \left. + v_3 \frac{\partial}{\partial\theta} P_3(\cos\theta)\right] dt\, d\phi \\
& + 2\sin\theta \left[w_2 \frac{\partial}{\partial\theta} P_2(\cos\theta) + w_3 \frac{\partial}{\partial\theta} P_3(\cos\theta)\right] dr\, d\phi. \quad (A1)
\end{aligned}
$$

The perturbed quantities $(h_i(r), m_i(r), m_i(r), k_i(r))$ $(i = 0, 2)$ and $(i_i(r), v_i(r) i_i(r))$ $(i = 1, 2, 3)$ are found by solving the linearized Einstein equations

$$
\delta G_{\mu\nu} = 8\pi \delta T_{\mu\nu}. \quad (A2)
$$

The pressure p and the energy density ρ can be expanded as $p = p^{(0)} + \delta p$, $\rho = \rho^{(0)} + \delta\rho$, with

$$
\delta p(r, \theta) = \delta p_0 + \delta p_2 P_2(\cos\theta), \quad (A3)
$$

$$
\delta \rho(r, \theta) = \frac{\rho^{(0)\prime}}{P^{(0)\prime}}[\delta p_0 + \delta p_2 P_2(\cos\theta)]. \quad (A4)
$$

A1 Deformation induced by a dipole ($l = 1$) magnetic field

As discussed in Section 2.3, $a(r, \theta) = a_1(r)P_1(\cos\theta)$; by expanding the components (rr), $(r\theta)$, $(\theta\theta) - \sin^{-2}\theta(\phi\phi)$ of the perturbed Einstein equation (A2) in spherical, tensor harmonics and by considering the $l = 2$ equations, which give the stellar deformation, we have (Ioka & Sasaki 2004)

$$
\begin{aligned}
& h_2' + \frac{4e^\lambda}{\nu' r^2} y_2 + \left[\nu' - \frac{8\pi e^\lambda}{\nu'}\left(p^{(0)} + \rho^{(0)}\right) + \frac{2}{r^2\nu'}(e^\lambda - 1)\right] h_2 \\
& \quad = \frac{\nu'}{3} e^{-\lambda} a_1'^2 + \frac{4}{3r^2} a_1 a_1' \\
& \qquad + \frac{1}{3}\left(-\nu' + \frac{2}{\nu' r^2} e^\lambda\right) \zeta^2 e^{-\nu}(a_1)^2 - \frac{16\pi}{3\nu' r^2} e^\lambda j_1 a_1, \quad (A5)
\end{aligned}
$$

$$
\begin{aligned}
& y_2' + \nu' h_2 = \frac{\nu'}{2} e^{-\lambda} a_1'^2 \\
& \quad + \frac{1}{3}\left[\frac{e^{-\lambda}}{r}\left(\nu' + \lambda' + \frac{2}{r}\right) + e^{-\nu}\zeta^2 - \frac{2}{r^2}\right] a_1 a_1' \\
& \quad - \frac{\nu'}{3} e^{-\nu}\zeta^2 a_1^2 - \frac{4\pi}{3} j_1 \left(a_1' + \frac{2}{r} a_1\right), \quad (A6)
\end{aligned}
$$

where $j_1 = c_0(\rho + p)r^2$ and

$$
y_2 \equiv h_2 + k_2 - \frac{e^{-\lambda}}{6} a_1'^2 - \frac{2e^{-\lambda}}{3r} a_1 a_1' - \frac{2}{3r^2} a_1^2. \quad (A7)
$$

Assuming regularity of h_2 and y_2 as $r \to 0$ implies that near the origin

$$
h_2 \simeq Ar^2, \quad y_2 \simeq Br^4, \quad (A8)
$$

where

$$B = \left(-2\pi A + \frac{16}{3}\pi\alpha_0^2\right)\left(p_c^{(0)} + \frac{\rho_c^{(0)}}{3}\right)$$
$$- \frac{4\pi}{3}\alpha_0 c_0\left(\rho_c^{(0)} + p_c^{(0)}\right) + \frac{\alpha_0^2\zeta^2}{6e^{\nu_c}}. \tag{A9}$$

It is worth mentioning that the terms in a_1, a_1' which appear in the definition of y_2 equation (A7) are important: if they are not included (i.e. if we define $y_2 \equiv h_2 + k_2$), the asymptotic behaviour (A8) is not satisfied.

The quantities h_2, y_2 inside the star can be decomposed as follows:

$$h_2 = c_1 h_2^h + h_2^p,$$
$$y_2 = c_1 y_2^h + y_2^p. \tag{A10}$$

For magnetic fields extending throughout the star, h_2^p and y_2^p can be found by integrating (A5), (A6) from $r = 0$ with, for instance, $A = 1$ and B given by (A9); h_2^h and y_2^h are the solutions of the associated homogeneous equations (i.e. with $a_1 = a_1' = 0$).

When the magnetic field is confined to the crust, in the core (defined conventionally by $0 \leqslant r \leqslant r_c$) $a_1 \equiv 0$, and equations (A5), (A6) are homogeneous; thus in this region $h_2 = h_2^h$, $y_2 = y_2^h$. On the crust–core interface $r = r_c$, we impose $a_1 = 0, a_1' = $ constant. We integrate the non-homogeneous equations starting at $r = r_c$ with the initial conditions

$$h_2^p(r_c) = 0, \quad y_2^p(r_c) = -\frac{e^{-\lambda(r_c)}}{6}[a_1'(r_c)]^2. \tag{A11}$$

The non-vanishing value for $y_2^p(r_c)$ follows from the requirement of continuity of $h_2 + k_2$ at the crust–core interface (see equation A7).

The constant c_1 in (A10) can be determined by matching the solution inside the star with the analytical solution in vacuum (Konno et al. 1999):

$$h_2 = K Q_2^2(z) + \hat{h}_2(z)$$
$$y_2 = -\frac{2K}{\sqrt{z^2-1}}Q_2^1(z) + \hat{y}_2(z) - \frac{e^{-\lambda}}{6}(a_1')^2$$
$$- \frac{2}{3r}e^{-\lambda}(a_1' a_1) - \frac{2}{3r^2}(a_1)^2. \tag{A12}$$

Here K is an integration constant, $a_1(r)$ is given by equation (76):

$$a_1 = -\frac{3\mu}{8M^3}r^2\left[\ln\left(1 - \frac{2M}{r}\right) + \frac{2M}{r} + \frac{2M^2}{r^2}\right], \tag{A13}$$

Q_m^n are the associated Legendre functions of the second kind:

$$Q_2^2(z) \equiv \frac{z(5-3z^2)}{z^2-1} + \frac{3}{2}(z^2-1)\ln\left(\frac{z+1}{z-1}\right), \tag{A14}$$

$$Q_2^1(z) \equiv \frac{2-3z^2}{\sqrt{z^2-1}} + \frac{3}{2}z(\sqrt{z^2-1})\ln\left(\frac{z+1}{z-1}\right), \tag{A15}$$

with $z \equiv \frac{r}{M} - 1$, and

$$\hat{y}_2 \equiv \frac{3\mu^2}{8M^4}\frac{7z^2-4}{z^2-1} + \frac{3\mu^2}{16M^4}\frac{z(11z^2-7)}{z^2-1}\ln\left(\frac{z-1}{z+1}\right)$$
$$+ \frac{3\mu^2}{16M^4}(2z^2+1)\left(\ln\frac{z-1}{z+1}\right)^2, \tag{A16}$$

$$\hat{h}_2 \equiv -\frac{3\mu^2}{16M^4}\left[3z - \frac{4z^2+2z}{z^2-1}\right]$$
$$- \frac{3\mu^2}{32M^4}\left[3z^2 - 8z - 3 - \frac{8}{z^2-1}\right]\ln\left(\frac{z-1}{z+1}\right)$$
$$+ \frac{3\mu^2}{16M^4}(z^2-1)\left(\ln\frac{z-1}{z+1}\right)^2. \tag{A17}$$

We have checked, both analytically and numerically, that (A12) is actually solution of (A5), (A6) in vacuum. Matching h_2 and y_2 at $r = R$ allows us to fix the constants c_1 and K.

The integration constant K is related to the mass–energy quadrupole moment of the star (see Section 2.5) by the relation

$$K = \frac{5Q}{8M^3} + \frac{3\mu^2}{4M^4}. \tag{A18}$$

Indeed, the asymptotic limit of $h_2(r)$ for $r \to \infty$ is

$$h_2 \to \frac{Q}{r^3}. \tag{A19}$$

Finally, we can compute the surface ellipticity of the star (80) following the definitions of Chandrasekhar & Miller (1974) and Konno et al. (1999):

$$e_{\mathrm{surf}} = -\frac{3}{2}\left(\frac{\delta r_2}{r} - k_2\right) = -\frac{3}{2}\left(\frac{\delta p_2}{rp^{(0)\prime}} - k_2\right)$$
$$= \left(-\frac{2c_0 a_1}{r\nu'} + \frac{3h_2}{r\nu'} - \frac{3k_2}{2}\right)_{r=R}, \tag{A20}$$

where $\delta p = \sum_l \delta p_l P_l$, $\delta r = \sum_l \delta r_l P_l$ and

$$\delta p_2 = -\left(\rho^{(0)} + p^{(0)}\right)h_2 + \frac{2}{3r^2}a_1 j_1. \tag{A21}$$

Relation (A21) is a consequence of Euler equation. Indeed, from equations (52), (53), (56), it follows that

$$\ln\left(\sqrt{-g_{00}}\frac{\rho+p}{n}\right) = c_0\sin\theta a_{,\theta} + \mathrm{constant}. \tag{A22}$$

If we perturb (A22), using the following relation which holds for a barotropic EOS

$$\delta p = n\delta\left(\frac{\rho+p}{n}\right),$$

we find (A21).

A2 Deformations induced by a quadrupole ($l = 2$) magnetic field

We assume $a(r,\theta) = a_2(r)P_2(\cos\theta)$, and expand in spherical, tensor harmonics the (rr)-, $(r\theta)$-, $(\theta\theta) - \sin^{-2}\theta(\phi\phi)$-components of the perturbed Einstein equation (A2). We find that the $l = 2$ equations are

$$h_2' + \frac{4e^\lambda}{\nu' r^2}y_2 + \left[\nu' - \frac{8\pi e^\lambda}{\nu'}\left(p^{(0)}+\rho^{(0)}\right) + \frac{2}{r^2\nu'}(e^\lambda-1)\right]h_2$$
$$= \frac{3}{7}\nu' e^{-\lambda}a_2'^2 + \frac{12}{7r^2}a_2 a_2' - \frac{3}{7}\left(\nu' + \frac{2}{\nu' r^2}e^\lambda\right)\zeta^2 e^{-\nu}(a_2)^2, \tag{A23}$$

$$y_2' + \nu' h_2 = \frac{3}{14}\nu' e^{-\lambda}a_2'^2$$
$$+ \frac{3}{7}\left[\frac{e^{-\lambda}}{r}\left(\nu' + \lambda' + \frac{2}{r}\right) - \frac{3}{7}e^{-\nu}\zeta^2 - \frac{2}{r^2}\right]a_2 a_2'$$
$$- \frac{3}{7}\nu' e^{-\nu}\zeta^2 a_1^2, \tag{A24}$$

where we have defined

$$y_2 \equiv h_2 + k_2 + \frac{3}{14}e^{-\lambda}a_2'^2 - \frac{6e^{-\lambda}}{7r}a_2 a_2' - \frac{18}{7r^2}a_2^2. \tag{A25}$$

Assuming regularity of h_2 and y_2 as $r \to 0$ implies that near the origin

$$h_2 \simeq Ar^2 , \quad y_2 \simeq Br^4, \tag{A26}$$

where

$$B = -2\pi A \left(p_c^{(0)} + \frac{\rho_c^{(0)}}{3} \right). \tag{A27}$$

The integration of equations (A23), (A24) and the determination of Q and e_{surf} can be performed as in the previous section.

This paper has been typeset from a TeX/LaTeX file prepared by the author.